AMPERE Newsletter

Trends in RF and Microwave Heating

http://www.ampere-newsletter.org

Issue 98 **February 28, 2018**

INCLUDING SELECTED MD-10 PAPERS

In this Issue: **Page**

ISSN 1361-8598

Localized Microwave-Heating (LMH) and the Matthew Effect

Eli Jerby
Faculty of Engineering, Tel Aviv University, Israel
E-mail: jerby@eng.tau.ac.il

1 Matthew effect

The term Matthew effect, coined by Merton in 1968 [1], represents a universal principle, also known as the accumulated effect of advantages and disadvantages. It explains a variety of different phenomena in diverse scientific areas, and in daily life as well. In particular, various appearances of the Matthew effect in human societies are well characterized in social sciences and humanities, including economics, sociology, theology and education [2]. Referred to Matthew the Apostle who lived in the first century, the eternal wonderment: "Why the rich get richer and the poor get poorer?" [3] has raised one of the ethical dilemmas reflected in this principle, since the biblical profits till our own era and the contemporary globalization issues [4].

In academic life [1], the Matthew effect is clearly seen in the ways that academic prestige (as an asset) is accumulated, and tends to further evolve in distinct focal points considered as centers of excellence. These are for instance the (relatively few) élite academic institutions, which attract a growing number of excellent students from all over the world, and hence continuously elevate their acceptance criteria (and further escalate their attraction and reputation). Another example is the top-ranked scientific Journals, which become more and more desired by many authors, and consequently receive a growing number of submissions and citations (which lead, as a positive feedback, to a further increase of their rejection rates, and hence inflates their scientific ranking).

The system of academic metrics, using over-simplified indices of merit (e.g. impact factors and *h* indices), is not only a means to measure quality, but actually an accelerator for the unstable dynamics associated with this trend, pretended to be a desire for excellence. One of the destructive aspects of the same Matthew-effect mechanism is the continuous deterioration and actually the suppression of the larger middle-class communities of the seemingly mediocre entities (either ordinary people, or second-world countries, or even some glory-less but essential professional and academic organs).

The Matthew effect also impedes the evolution of microwave-heating R&D societies as independent professional communities. One of the expressions of this growing barrier is the increasing difficulties in publishing a Journal dedicated to this niche field (with an inherently lower impact factor).

The universal mechanism of Matthew effect also underlies one of the physical phenomenon of our interest, namely the localized microwave heating (LMH) and hotspot formation. This article presents therefore the LMH paradigm in an analogy to the Matthew effect, and shows the hotspot formation as an accumulated effect of advantages and disadvantages in relation to microwave heating. Several examples and potential applications of this mechanism are reviewed.

2 Localized microwave-heating (LMH)

Microwave heating is commonly utilized in uniformly-distributed volumetric schemes, such as ovens, belt applicators, and furnaces [5]. The heat-affected zone (HAZ) is typically comparable to the microwave wavelength, in the order of $\sim 10^{-1}$ m. Non-uniform heating patterns may accidentally evolve in such processes, hence rapidly creating local hotspots with significantly high local temperatures. Such localization effects could be harmful in microwave applications that require uniform heating, such as food processing and drying.

The localized microwave-heating (LMH) effect is intentionally utilized (e.g. by microwave drills [6]) by purposely exciting a thermal-runaway instability [7, 8], which generates a hotspot with a sub-wavelength HAZ (in the order of $\sim 10^{-3}$ m). LMH may occur in materials characterized by temperature-dependent properties, which dictate a faster rate of energy absorption than diffusion [9]. It enables a local temperature increase to above 1,000ºC in a

heating rate of >100ºC/s in various materials. The LMH instability is ceased at the material's phase transition, to liquid, gas, or plasma.

The LMH paradigm [10,11], embodied in the microwave-drill concept, is effectively extended for various other applications. LMH effects have been demonstrated in various materials [12], including concrete [13,14], ceramics [15,16], and basalts [17,18]. LMH may also be useful for microwave-assisted mining [19] and concrete-recycling [20] applications. It was also found applicable for glass [21], polymers [22], and silicon [23,24]. A doping effect induced in silicon by LMH was also demonstrated [25]. In this experiment, silver and aluminum dopants were locally diffused by LMH into silicon to form a diode PN-junction.

LMH is also studied for medical applications such as tissue heating [26], bone drilling [27], interstitial treatments [28,29], ablation therapy [30], and DNA amplification [31]. Open-end coaxial applicators are used for direct heating of liquids and for activation of chemical reactions [32,33]. LMH may generate plasmoids, directly from solid substrates [34-36], and produce nano-particles [37-39].

Due to the significant energy concentration, the LMH effect can be implemented by a relatively low power (in the order of ~0.1 kW). This feature has led to the development of solid-state LMH applicators [21]. Consequently, the LMH paradigm is also extended to compact microwave heaters, and to new applications such as incremental sintering of metal powders for 3-D printing and additive manufacturing [40], ignition of thermite reactions for material processing and combustion [41] (also in oxygen-free environments such as underwater [42,43] or in space), and to material identification by breakdown spectroscopy (MIBS) [44].

3 The LMH instability as an accumulative effect

The LMH instability can be explained in a figurative manner, as illustrated in Fig. 1 [10]. The open-end applicator is applied to a material of which the dielectric loss factor tends to increase, and the thermal conductivity tends to decrease with temperature. The initial heating of the (originally) uniform material increases the temperature near the electrode tip, hence the spatial distributions of the material properties vary accordingly. The loss factor increases in this vicinity (and the thermal conductivity decreases there), hence more and more power is absorbed there, which leads to an unstable LMH response. This process illustrates the Matthew effect as well. The directed radiation-pattern creates a local "initial advantage" which causes the material there to modify its local properties in a way that further enhances and increases the initial advantage. This positive feedback leads to a confined hotspot.

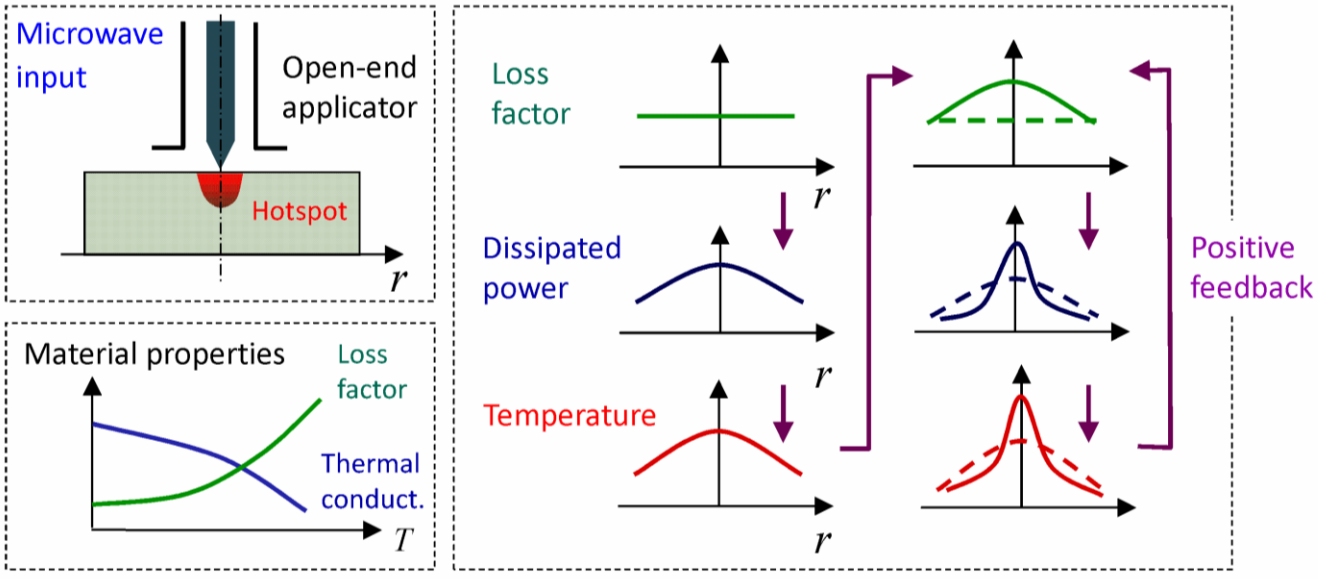

Figure 1: The induced thermal-runaway instability as an accumulated effect [10].

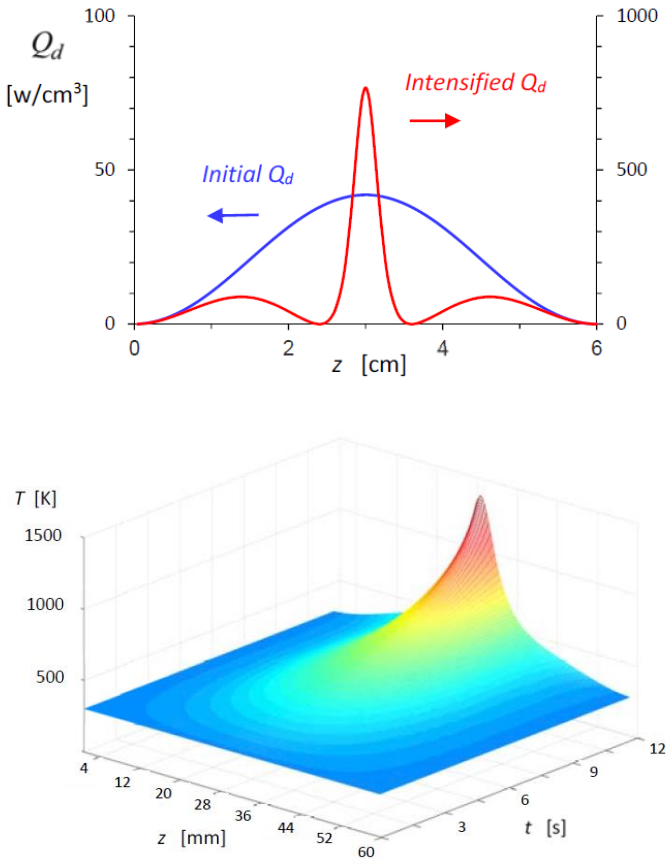

Figure 2: A numerical example of an accumulative LMH effect in a 1-D cavity [11]: (top) The initial and final profiles of the dissipated power density Q_d along the cavity, from a sine-squared to a sharper profile. (bottom) The localized temperature profile along the cavity, and the hotspot evolved.

As an example for the LMH intensification effect, Ref. [11] shows a model of a 1-D resonator filled with a dielectric medium. The complex dielectric constant $\varepsilon_r(T)$ has nearly parabolic temperature dependence as illustrated in Fig. 1. The ~6-cm long resonator is excited by a 2.45-GHz, ~1 kW power, at the fundamental axial mode. The coupled solution of the wave and heat equations shows that higher-order modes are dynamically evolved during the non-uniform microwave heating [11]. The temperature-dependent dielectric permittivity is being modified along the resonator, and coupled to the higher-order modes. This mode dynamics modifies the EM dissipated power $Q_d(z,t)$ initially distributed as the original fundamental-mode (sine-squared) profile. As the LMH instability proceeds, Q_d becomes significantly intensified and confined at the sub-wavelength hotspot region, as shown in Fig. 2 (top). The temperature rise is accelerated, and its localized profile is sharpened accordingly, hence the hotspot is intensified as shown in Fig. 2 (bottom).

In another example [10], a similar arbitrary material is placed in front of a waveguide aperture. The LMH effect is seen in Fig. 3 by the temperature profile and also by the focusing-like convergence of the Poynting vector towards the hotspot. This focusing also demonstrates the negative aspect of the Matthew effect, namely the suppression of the depleted vicinity surrounding the favorite spot.

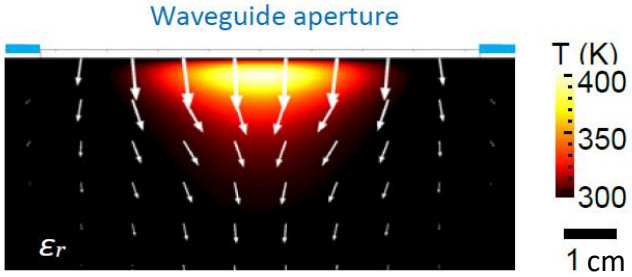

Figure 3: A numerical simulation of a hotspot evolved in an arbitrary material placed in front of a waveguide aperture [10]. The LMH effect is evident by the temperature profile, as well as the focusing-like convergence of the Poynting vector (denoted by the white arrows).

4 The microwave drill

An example of a practical LMH implementation is for instance a silent microwave-drill developed for concrete [14] (capable of drilling >25-cm deep, 12-mm diameter holes). More delicate microwave drilling operations were also demonstrated in ~1-mm diameter, for instance by relatively low-power (~0.1 kW) LMH applied to soda-lime glass plates (of 1-4 mm thickness) [21]. A simulation of the LMH evolution in these cases agrees well with the experimental measurements. Figure 4 shows for instance a simulated hotspot profile, and an LMH-drilled hole in glass [21].

The relatively low power needed for open-end coaxial applicators to reach LMH intensification in millimeter scales (typically below ~0.2 kW) makes solid-state generators (e.g. LDMOS [21]) suitable as sources for LMH applicators. These compact schemes enable a new range of portable LMH intensifiers.

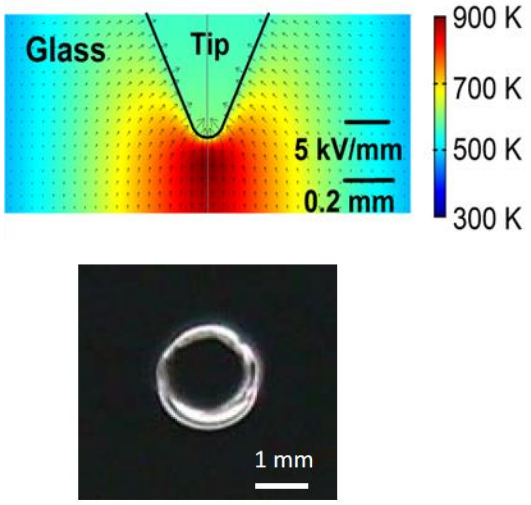

Figure 4: LMH effect in glass irradiated by a coaxial open-end applicator using an LDMOS-based microwave-drill [21]: (top) The simulated spatial temperature and electric-field distributions at the hotspot, and (bottom) a ~1.6-mm$^{\emptyset}$ hole made by LMH in glass.

5 Plasma ejection from solids

Dusty plasmas in forms of fireballs and fire-columns as shown in Fig. 5 can be ejected by LMH directly from hotspots evolved in solid substrates made of various dielectric and metallic materials [34-39]. The LMH-plasma process begins with a hotspot formation as in microwave drilling. For plasma ejection however, the electrode is lifted up (rather than pushed in) in order to detach the molten drop from the surface, and to further inflate it to a form of a buoyant fireball.

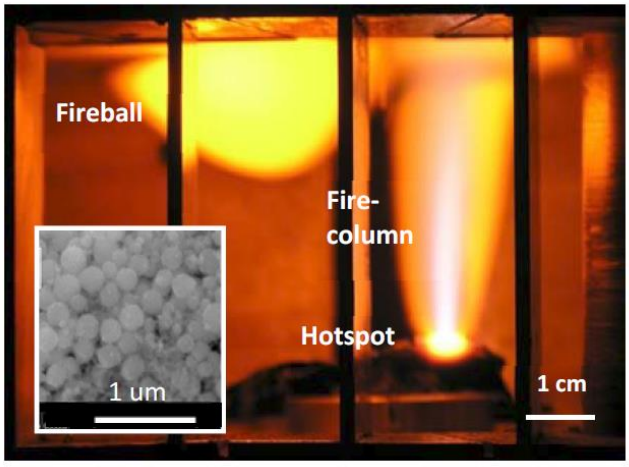

Figure 5: Plasmoids ejected by LMH from a hotspot in glass [35,36]: The hotspot in the solid substrate, the fire-column ejected, and the secondary fireball evolved. The inset shows nano-particles produced by LMH generated dusty plasma.

Beside their resemblance to natural ball-lightning phenomena, fireballs and fire-columns as shown in Fig. 5, may also have practical importance, e.g. as means to produce nano-particles directly from various substrate materials, such as silicon, glass, ceramics, copper, and titanium [35-39]. Nanoparticles were observed in these and other materials, both by in-situ synchrotron small-angle X-ray scattering (SAXS) of the dusty plasma, and by ex-situ SEM observations of the nano-powders collected after the processes. Particle of various sizes, shapes, and number densities have been obtained (typically of <0.1 μm size and ~10^{16} m^{-3} number density within the dusty plasma). The LMH generated plasma can also be used for material identification [44] by atomic emission spectroscopy of the light emitted by the plasma ejected from the hotspot (similarly to the laser induced breakdown spectroscopy (LIBS)).

6 Doping and surface treatment by LMH

The feasibility of local doping of silicon by silver and aluminum using an LMH process was demonstrated in experiments in which the dopant material was incorporated in the electrode tip [25]. Its diffusion into the locally heated bulk was utilized in order to form a sub-micron junction. The doping depth was determined by the applied microwave power. Oxidation effects were also observed in these experiments, conducted in air atmosphere.

Chemical reactions excited by LMH for surface treatment also include thermite reactions for rust conversion to iron [41]. These LMH techniques open new possibilities for a variety of surface treatments and local surface processing.

7 LMH of metal powders

Coupling mechanisms of microwaves and metal powders are known in the literature in various volumetric schemes [45]. Experiments also show that metal powders with negligible dielectric losses can be effectively heated, and incrementally solidified by localized microwaves [40]. This LMH effect is attributed to the magnetic component of the EM field, and to the eddy currents induced in the metal-powder particles, as illustrated in Fig. 6 [45]. This effect, intensified by the micro-powder geometry, also occurs in diamagnetic metals such as

copper. The heat is generated due to the metal electric resistivity, which impedes the eddy currents. This magnetic-like LMH effect is not characterized by thermal-runaway instability since the temperature tends to stabilize at ~700 K due to the particle necking and consolidation.

8 LMH ignition of thermite reactions

Powder mixtures, such as pure aluminum and magnetite powders, may generate energetic thermite reactions. These reactions are useful for a variety of combustion and material processing applications. However, the usage of these reactions is yet limited by the difficult ignition. We found that an easier ignition of thermite reactions as in Fig. 6 (right) is feasible by intensified LMH [41]. The power required for thermite ignition by LMH is ~0.1 kW for a ~3-s period, provided by a solid-state microwave generator. These experiments also demonstrate the feasibility of cutting and welding by relatively low-power LMH.

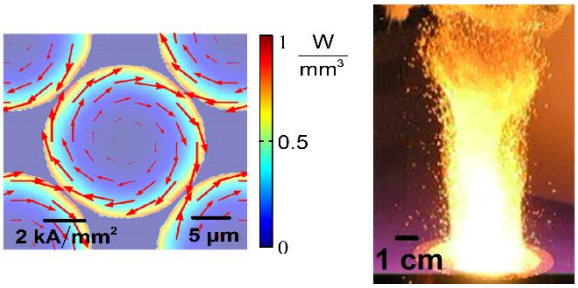

Figure 6: LMH of metallic powders: (left) Eddy currents induced in copper powder [45]. (right) A thermite flame ignited by LMH [41].

Due to their zero-oxygen balance, exothermic thermite reactions may also occur underwater. However, this feature is also difficult to utilize because of the hydrophobic properties of the thermite powder. The bubble-marble (BM) effect [42] enables the insertion and confinement of a thermite-powder batch into water by a static magnetic field, and its ignition by LMH underwater [43]. Potential applications of this underwater combustion may include wet welding, thermal drilling, detonation, thrust generation, material processing, and composite-material production. These are applicable to other oxygen-free environments as well, such as the outer space.

9 LMH potential for 3D printing

The LMH effect in metal powders is also associated with internal micro-plasma breakdowns between the particles, which leads to local melting and solidification of the metal powder. This effect enables a potential technique for stepwise 3D printing and additive manufacturing (AM) [40]. The solidified drop of metal powder is placed in this technique as a building block on top of the previously constructed block in a stepwise AM process, illustrated in Fig. 7a. A rod constructed by LMH-AM from bronze-based powder is shown in Fig. 7b [40]. Magnetic fixation of iron powder for LMH-AM was also demonstrated [46].

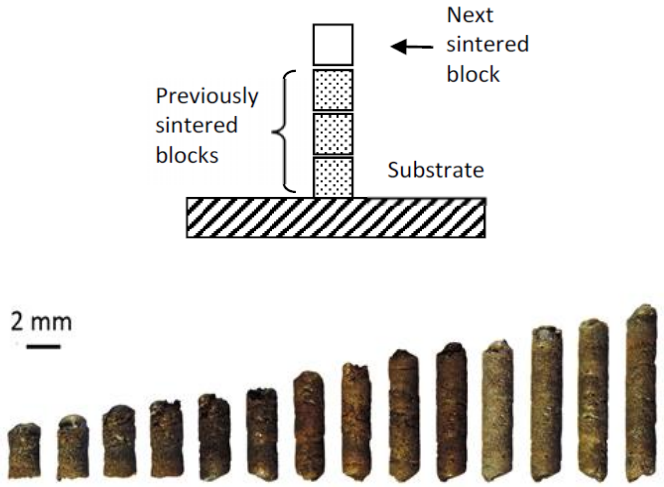

Figure 7: Additive manufacturing (3D printing) of metal powders by LMH [40]: (top) A conceptual scheme of the stepwise LMH-AM process. (bottom) A 2-mm$^{\phi}$ rod constructed in 14 consequent steps from bronze-based powder.

10 Discussion

The LMH paradigm, presented here in the context of Matthew effect, enables microwave heating in HAZ sizes much smaller than the microwave wavelength. The microwave radiation is self-focused intentionally into a millimeter-size hotspot. Further to melting and evaporation, dusty plasma rich of nanoparticles can also be directly ejected from the hotspot.

The LMH paradigm incorporates the theory of induced thermal-runaway instability together with experimental studies and various applications. LMH is applicable to dielectrics and metals as well (in solid and powder forms), and to biological tissues.

Figure 8 shows a conceptual scheme of the LMH relevance to solid, powder and plasma states, as well as their transitions and related applications.

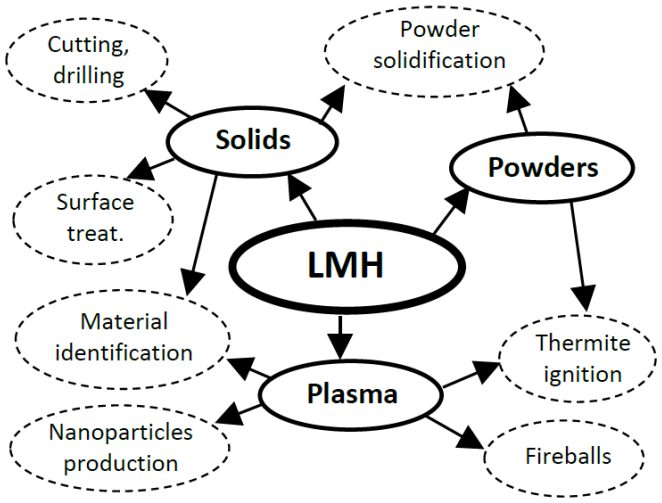

Figure 8: The LMH relevance to solid, powder and plasma states; their transitions, and related applications [10].

The LMH paradigm is presented here in the wider context of the Matthew effect. The intuitive analogy illustrated here may provide a better insight of the LMH instability, and a non-mathematical heuristic explanation of its non-linear dynamics. For those who are interested in Matthew effects in other disciplines, the LMH phenomena and hotspot formation may provide a visual demonstration of the accumulated effect of advantages and disadvantages. In particular, the damage caused by unintentional LMH may exemplify the destructive potential of Matthew effects, e.g. to the contemporary academic system and to the society in general.

Acknowledgements

The LMH research reviewed in this article was supported in part by The Israel Science Foundation (Grant Nos. 1270/04, 1639/11, and 1896/16). The LMH similarity to Matthew effect was identified in conversations with my wife, Dr. Iris Jerby, about her sociological and educational studies.

For further reading

1. R. K. Merton, "The Matthew effect in science" *Science*, 1968, **159**, 56–63.
2. The article "Matthew effect" in Wikipedia, and references therein
3. Matthew 13:12 "For whosoever hath, to him shall be given, and he shall have abundance: but whosoever hath not, from him shall be taken away even that which he hath."
4. Anand Giridharadas, *Winners Take All - The Elite Charade of Changing the World*, Alfred A. Knopf, New York, 2018.
5. A. C. Metaxas, *Foundations of Electroheat—A Unified Approach*, Chichester, U.K.: Wiley, 1996.
6. E. Jerby, V. Dikhtyar, O. Actushev and U. Grosglick, "The microwave drill," *Science*, 2002, **298**, 587-589.
7. G. Roussy, A. Bennani, J. Thiebaut, "Temperature runaway of microwave irradiated materials," *Jour. Appl. Phys*., 1987, **62**, 1167-1170.
8. E. Jerby, O. Aktushev, V. Dikhtyar, "Theoretical analysis of the microwave-drill near-field localized heating effect," *Jour. Appl. Phys.*, 2005, **97**, Art. No. 034909, 1-7.
9. Y. Alpert, E. Jerby, "Coupled thermal-electromagnetic model for microwave heating of temperature-dependent dielectric media," *IEEE Trans. Plas. Sci.*, 1999, **27**, 555-562.
10. Y. Meir, E. Jerby, "The localized microwave-heating (LMH) paradigm – Theory, experiments, and applications," Proc. 2nd Global Congress on Microwave-Energy Applications, 2GCMEA, pp. 131-145, Long Beach, California, July 23-27, 2012; Also in Proc. AMPERE 2015, Krakow, Poland, Sept. 14-17, 2015.
11. E. Jerby, "Localized microwave-heating intensification – A 1-D model and potential applications," *Chemical Engineering and Processes (CEP)*, 2017, **122**, 331-338.
12. E. Jerby, O. Aktushev, V. Dikhtyar, P. Livshits, A. Anaton, T. Yacoby, A. Flax, A. Inberg, D. Armoni, "Microwave drill applications for concrete, glass and silicon" Proc. 4th World Congress Microwave & Radio-Frequency Applications, 156-165, Nov. 4-7, 2004, Austin, Texas.
13. E. Jerby, V. Dikhtyar, "Drilling into hard non-conductive materials by localized microwave radiation," 8th Int'l Conf. Microwave & High-Frequency Heating, Bayreuth, Sept. 4-7, 2001, in *Advances in Microwave and Radio-Frequency Processing*, M. Willert-Porada, Ed., Springer, 2006, 687-694.
14. E. Jerby, Y. Meir, Y. Nerovny, O. Korin, R. Peleg, Y. Shamir, "Silent microwave-drill for concrete," *IEEE Trans. Microwave Theory Tech.*, 2018, **66**, 522-529.
15. E. Jerby, V. Dikhtyar, O. Aktushev, "Microwave drill for ceramics," *Amer. Ceram. Soc. Bull.*, 2003, **82**, 35-37.
16. E. Jerby, A.M. Thompson, "Microwave drilling of ceramic thermal barrier coatings," *Jour. Amer. Ceram. Soc.*, 2004, **87**, 308-310.
17. E. Jerby, Y. Meir, M. Faran, "Basalt melting by localized-microwave thermal-runaway instability," Proc. AMPERE 14th Int'l Conf. Microwave & High Frequency Heating, 255-258, Nottingham, UK, Sept. 16-19, 2013.
18. E. Jerby, Y. Shoshany, "Fire-column-like dusty-plasma ejected from basalt by localized microwaves," 45 IEEE Int'l Conf. on Plasma Sciences, ICOPS-2018, Denver, Colorado, June 24-28, 2018; also in MD-10 Proc., 151-157, Ed. Yu. A Lebedev, Yanus-K, Moscow, 2018.

19. G. Wang, P. Radziszewski, J. Ouellet, "Particle modeling simulation of thermal effects on ore breakage," *Comput. Mater. Sci.*,2008, **43**, 892–901.
20. N. R. Lippiatt, F. S. Bourgeois, "Recycling-oriented investigation of local porosity changes in microwave heated-concrete," *KONA Powder & Particle Jour.*, 2014, **31**, 247-264.
21. Y. Meir and E. Jerby, "Localized rapid heating by low-power solid-state microwave-drill," *IEEE Trans. Microwave Theory & Tech.*, 2012, **60**, 2665-2672.
22. J. B. A. Mitchell, E. Jerby, Y. Shamir, Y. Meir, J. L. LeGarrec, M. Sztucki, "Rapid internal bubble formation in a microwave heated polymer observed in real-time by X-ray scattering," *Polym. Degradation Stab.*, 2011, **96**, 1788-1792.
23. X. Wang, W. Liu, H. Zhang, S. Liu, Z. Gan, "Application of microwave drilling to electronic ceramics machining," 7th Int'l Conf. Electronics Packaging Technology, Proc. Article # 4198945, pp. 1-4, Aug. 26-29, 2006, Shanghai, China.
24. R. Herskowits, P. Livshits, S. Stepanov, O. Aktushev, S. Ruschin, E. Jerby, "Silicon heating by a microwave-drill applicator with optical interferometric thermometry," *Semicond. Sci. Tech.*, 2007, **22**, 863-869.
25. P. Livshits, V. Dikhtyar, A. Inberg, A. Shahadi, E. Jerby, "Silicon doping by a point-contact microwave applicator," *Microelectron. Eng.*, 2011, **88**, 2831-2836.
26. A. Copty, F. Sakran, M. Golosovsky, D. Davidov, A. Frenkel, "Low power near-field microwave applicator for localized heating of soft matter", *Appl. Phys. Lett.*, 2004, **84**, 5109–5111.
27. Y. Eshet, R. Mann, A. Anaton, T. Yacoby, A. Gefen, E. Jerby, "Microwave drilling of bones," *IEEE Trans. Biomedical Eng.*, 2006, **53**, 1174-1182.
28. T. Z. Wong, B. S. Trembly, "A theoretical model for input impedance of interstitial microwave antennas with choke," *Int. Jour. Radiat. Oncol. Biol. Phys.*, 1994, **28**, 673-682.
29. I. Longo, G. B. Gentili, M. Cerretelli, N. Tosoratti, "A coaxial antenna with miniaturized choke for minimally invasive interstitial heating," *IEEE Trans. Biomed. Eng.*, 2003, **50**, 82-88.
30. P. Keangin, P. Rattanadecho, "Analysis of heat transport on local thermal non-equilibrium in porous liver during microwave ablation," *Int'l Jour. Heat Mass Trans.*, 2013, **67**, 46–60.
31. A. Kempitiya, D. A. Borca-Tasciuc, H. S. Mohamed, M. M. Hella, "Localized microwave heating in micro-wells for parallel DNA amplification applications," *Appl. Phys. Lett.*, 2009, **94**, Art. No. 064106, 1-3.
32. F. Marken, "Chemical and electro-chemical applications of in situ microwave heating," *Annu. Rep. Prog. Chem., Sect. C*, 2008, **104**, 124–141.
33. Y. Tsukahara, A. Higashi,T. Yamauchi, T. Nakamura, M. Yasuda, A. Baba, Y. Wada, "In situ observation of nonequilibrium local heating as an origin of special effect of microwave on chemistry," *Jour. Phys. Chem. C*, 2010, **114**, 8965–8970.
34. V. Dikhtyar, E. Jerby, "Fireball ejection from a molten hot-spot to air by localized microwaves," *Phys. Rev. Lett.*, 2006, **96**, Art. No. 045002, 1-4.
35. Y. Meir, E. Jerby, Z. Barkay, D. Ashkenazi, J. B. A. Mitchell, T. Narayanan, N. Eliaz, J-L LeGarrec, M. Sztucki, O. Meshcheryakov, "Observations of ball-lightning-like plasmoids ejected from silicon by localized microwaves," *Materials*, 2013, **6**, 4011-4030.
36. E. Jerby, "Microwave-generated fireballs," *Encyclopedia of Plasma Technology*, Taylor and Francis, 2017, pp. 819-832.
37. J. B. Mitchell, J. L. LeGarrec, M. Sztucki, T. Narayanan, V. Dikhtyar, E. Jerby, "Evidence for nanoparticles in microwave-generated fireballs observed by synchrotron X-ray scattering," *Phys. Rev. Lett.*, 2008, **100**, Art. No. 065001, 1-4.
38. E. Jerby, A. Golts, Y. Shamir, S. Wonde, J. B. A. Mitchell, J. L. LeGarrec, T. Narayanan, M. Sztucki, D. Ashkenazi, Z. Barkay, "Nanoparticle plasma ejected directly from solid copper by localized microwaves," *Appl. Phys. Lett.*, 2009, **95**, Art. No. 191501.
39. S. Popescu, E. Jerby, Y. Meir, Z. Barkay, D. Ashkenazi, J. B. A. Mitchell, J-L. Le Garrec, T. Narayanan, "Plasma column and nano-powder generation from solid titanium by localized microwaves in air," *Jour. Appl. Phys.*, 2015, **118**, Art. No. 023302.
40. E. Jerby, Y. Meir, A. Salzberg, E. Aharoni, A. Levy, J. Planta Torralba and B. Cavallini, "Incremental metal-powder solidification by localized microwave-heating and its potential for additive manufacturing," *Additive Manufacturing*, 2015, **6**, 53-66.
41. Y. Meir, E. Jerby, "Thermite-powder ignition by electrically-coupled localized microwaves," *Combust. Flame*, 2012, **159**, 2474–2479.
42. Y. Meir, E. Jerby, "Insertion and confinement of hydrophobic metallic powder in water: The bubble-marble effect," *Phys. Rev. E*, 2014, **90**, Art. No. 030301(R), 1-4, 2014.
43. Y. Meir, E. Jerby, "Underwater microwave ignition of hydrophobic thermite powder enabled by the bubble-marble effect," *Appl. Phys. Lett*., 2015, **107**, Art. No. 054101, 1-4.
44. Y. Meir, E. Jerby, "Breakdown spectroscopy induced by localized microwaves for material identification," *Microw. Opt. Tech. Lett.*, 2011, **53**, 2281–2283.
45. T. Galek, K. Porath, E. Burkel, U. Van Rienen, "Extraction of effective permittivity and permeability of metallic powders in the microwave range," *Modell. Simul. Mater. Sci. Eng.*, 2010, **18**, Art. No. 025015, 1-13.
46. M. Fugenfirov, Y. Meir, A. Shelef, Y. Nerovni, E. Aharoni, E. Jerby, "Incremental solidification (towards 3D-Printing) of magnetically-confined metal-powder by localized microwave heating," *Int'l Jour. Comp. Math. Elect. Eng. (COMPEL)*, 2018, **37**, 1918-1932.

About the author

Eli Jerby received his Ph.D. degree in Electrical Engineering from Tel-Aviv University (TAU) in 1989. As a Rothschild and Fulbright post-doctoral fellow, he worked at MIT with the late Prof. George Bekefi on free-electron maser (FEM) and cyclotron-resonance maser (CRM) studies. Since his return to TAU in 1991 as a faculty member, Prof. Jerby has studied novel schemes of FEM's and CRM's, as well as localized microwave-heating effects and their applications (e.g. the microwave-drill invention, additive-manufacturing schemes), microwave-generated plasmas and fireballs, thermite reactions and metallic-fuel ignition by localized microwaves. Besides his scientific work, he has conducted in his TAU laboratory several projects for the industry, government, and start-up initiatives. Prof. Jerby served as a program committee member of int'l conferences and workshops in the fields of plasma, radiation sources, microwave heating, and microwave discharges. He also served as the Editor of JMPEE, the Journal of Microwave Power and Electromagnetic Energy (2006-2009) and of AMPERE Newsletter (2015-2017). More information and his publications are available at http://www.eng.tau.ac.il/~jerby

Space-Wave (Antenna) Radiation from the Wave Launcher (Surfatron) before the Development of the Plasma Column Sustained by the EM Surface Wave: A Source of Microwave Power Loss

Michel Moisan[1], Pierre Levif[1], Helena Nowakowska[2]

[1]Groupe de physique des plasmas, Université de Montréal, Montréal, Québec
[2] Institute of Fluid Flow Machinery, Polish Academy of Sciences, 80-952 Gdansk, Poland
Contact Email: michel.moisan@umontreal.ca

Abstract. As shown recently [1], whenever an electromagnetic (EM) surface wave (SW) sustains a plasma column, it is preceded by a non-guided wave over a short axial segment of the plasma column situated in the immediate vicinity of the wave launching structure. This wave can be regarded as a space wave since it spreads out microwave power into the free space, with a non-zero elevation angle (relative to the tube axis). Such a segment is akin to that of the near-field region of an antenna ending with the launching of the space wave. In that respect, coaxially surrounding the surface-wave discharge (SWD) with a circular waveguide (designated herein as a Faraday cage (FC)) under cut-off conditions eliminates, to some extent (depending on the FC length), the corresponding space-wave power loss. Such an outcome is first suggested by the fact that the plasma column length is observed to be longer when enclosed within a FC at cut-off. In fact, integrating the measured axial distribution of electron density along the plasma column leads to a larger number of electrons in the plasma column when enclosed in a FC at cut-off, demonstrating that additional EM power is then flowing along the plasma column. Modelling of the power loss due to space-wave radiation in open space is provided as a function of the length of the FC enclosing the plasma column. Even though the current work is centered on an SWD operated in argon at atmospheric pressure and at a field frequency of 915 MHz, some features are reported under different operating conditions (frequency, discharge tube diameter and gas pressure). It is observed that, for given operating conditions, the characteristic length of the space-wave radiation segment is constant and that its length decreases with increasing frequency; as a result, at 2450 MHz (wavelength in vacuum is 122 mm) depending on the wave launcher utilized, it extends from 3 to 28 mm only, possibly explaining why it has escaped the attention of researchers.

1 Introduction

An electric field with a high enough intensity can achieve the breakdown of a gas initially (electrically) neutral and sustain a discharge, yielding electrons and ions (charged particles), accompanied by remaining neutral atoms (molecules). Microwave (MW) electric fields are commonly used to generate plasmas: electrons (lighter particles) gain energy in the MW field and through collisions with heavy (essentially) neutral particles promoting the ionisation process. Among the various ways and methods of obtaining stable and reproducible MW plasmas, there is the propagation of an EM surface wave (SW) using the plasma column that it sustains and its surrounding dielectric tube as its guiding medium. Ionizing SWs can be launched with known devices such as surfatron and surfaguide. These can be considered to be small length antennas (relative to the EM wavelength in vacuum). Before the actual achievement of the SW plasma column, away from the launcher, there is an antenna near-field region close to it that yields at the end a non-guided space-wave radiation in the room, eventually detrimental to personnel and perturbing measurements. The current paper examines this problematic and discusses how to cope with it.

2 Characteristics of the space-wave radiation region preceding the development of a SW plasma column

2.1 Location and extent of the space-wave radiation region

Consider Figure 1 that schematically displays a current ***E***-field applicator used to achieve a tubular surface-wave discharge (SWD). The circular launching interstice (a 2–3 mm wide gap in the case of a surfatron) is the essential part needed for generating efficiently SW plasma columns. The electromagnetic (EM) field emerging from the interstice allows the establishment of a plasma column sustained by an EM surface wave in both directions from the gap. As illustrated in Figure 1, in

the case of the front column, the SWD commences at the power flow location marked $P(z_0)$, i.e., past the space-wave radiation region.

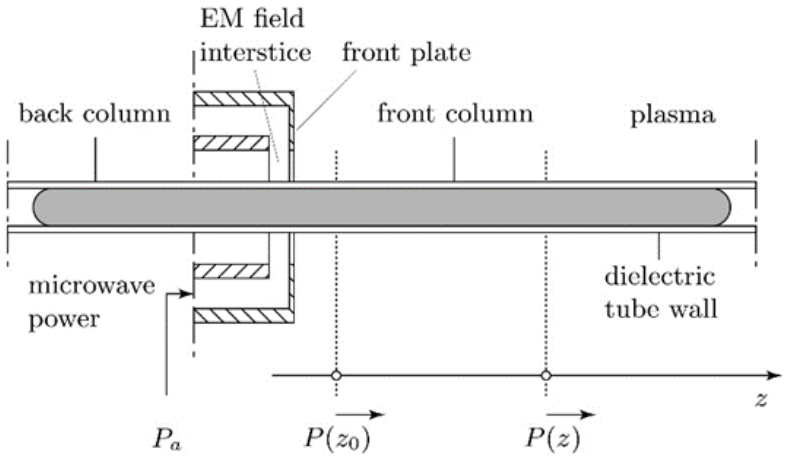

Figure 1: Schematic representation of an EM field applicator with a circular aperture such as used for achieving tubular SW discharges, highlighting its essential part, specifically the EM field interstice, typically forming in the case of a surfatron a 2–3 mm wide gap with a front plate 0.5 mm thick and edgy. As a result of the EM field emerging from the interstice in connection with microwave (absorbed) power P_a, a SW is launched in both directions (precisely past the $P(z_0)$ point for the front wave[1]), sustaining a plasma column inserted in a dielectric tube. The impedance matching system of the feed line with the power generator is not represented.

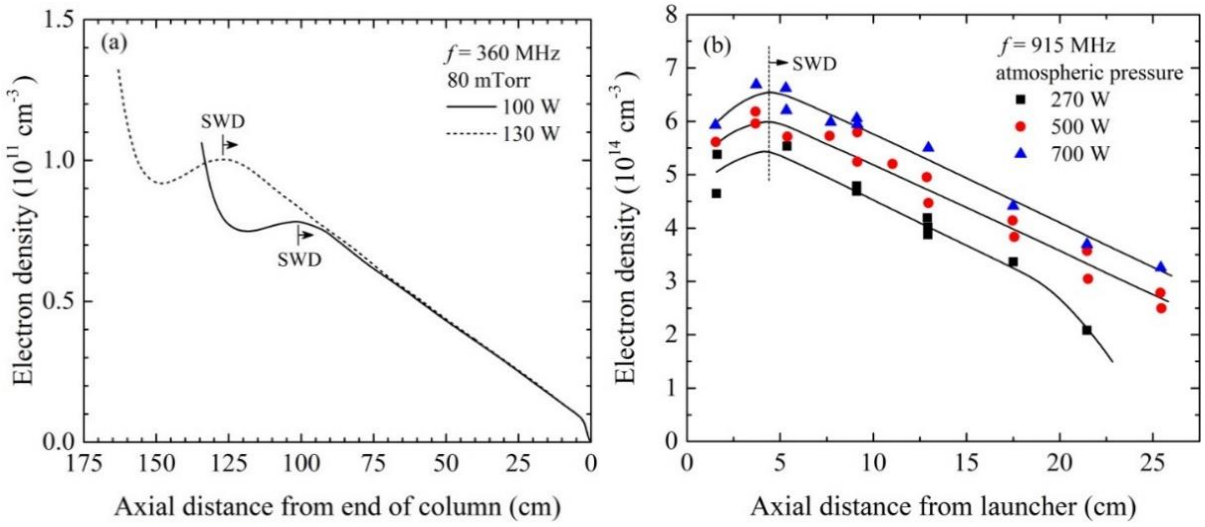

Figure 2 Radially averaged electron density measured along an argon SW plasma column sustained with a surfatron as a function of axial distance plotted: in (a) from the end of the plasma column of diameter 25 mm, at 80 mTorr (10.7 Pa) and at 360 MHz; the leftmost data point in the figure is situated at approximately 1–2 mm from the launcher interstice [2]; in (b) from the launcher aperture along a plasma column in a tube of 1.94 mm inner diameter, at atmospheric pressure and 915 MHz [3]. The SWD is open to free space in Figure 2(a) while, in Figure 2(b), it is inserted coaxially in a Faraday cage of radius R_{Fc} = 67.5 mm, much smaller than the minimum radius for wave cut-off in a cylindrical waveguide at 915 MHz[2], which is $R_{Fc(co)}$ = 96.1 mm.

[1] In the case of the back column emerging from the surfatron interstice, since it is partially enclosed within the surfatron body, the corresponding space-wave losses are eliminated by the surfatron body acting as a long enough FC (at cut-off).

[2] A circular waveguide enclosing (coaxially) at cut-off (on its fundamental mode) the plasma tube prevents waves from propagating within this conducting cage (but not the SW, which uses the discharge tube and the plasma as its propagating medium). The fundamental mode of a circular waveguide (i.e., the lowest frequency at which a wave can propagate within it) is the TE_{11} mode. Its corresponding wavelength is given by $\lambda_c = 2\pi R_{Fc(co)}/1.841$. At 915 MHz, a circular waveguide (Faraday cage) with a radius smaller than $R_{Fc(co)}$ = 96.1 mm is at cut-off, i.e., no wave can propagate within it. At 2450 MHz, $R_{Fc(co)}$ is 35.9 mm [4].

In Figure 2(a), which plots the axial distribution of electron density, the SWD starts developing down the plasma column from the point designated with an arrow. This assertion is based on the fact that the linear decrease of electron density that ensues is an essential attribute of SWDs (as discussed, for instance, in [1]). Concerning the plasma column region preceding the SWD, its main features, according to Figure 2(a), are: i) its axial extent and shape remain the same when microwave power is increased while its electron density increases accordingly; ii) the electron density and the intensity of the ***E***-field at the end of this plasma segment reach a relative maximum value that delineates the beginning of the SWD. The region nearest to the launcher is in fact related to the near-field region of an antenna[3] and, at its very end, EM power is radiated through a non-guided wave, designated as a *space wave*. In contrast, the SWD results from a SW guided along the plasma column axis. Similar observations (i and ii)) can be made with Figure 2(b), this time at a much higher frequency and at a higher gas pressure (atmospheric pressure), all measurements reported in the current paper having been carried out in argon discharges

2.2 *Properties of the radiation region observed near the opening made for the passageway of the discharge tube in a TM_{010} Beenakker cavity, an alternate device for achieving a tubular SWD*

A Beenakker cavity can be utilized as a SW ***E***-field applicator [5]. Figure 3 shows the axial variation, this time, of the intensity of the ***E***-field radial component of the microwave field detected with an electric-antenna radially oriented with respect to the discharge tube and with its tip situated at 2 mm away from the tube outer wall (to make sure detecting the SW radial field intensity, which radially decreases exponentially) [6]. The radiation field coming out from the cavity aperture reaches a maximum intensity value at approximately 17 mm from it, after which it decreases almost linearly. This maximum intensity is interpreted as being the location at which (or just before which) the space wave is generated and also as the beginning of the SWD. The fact that the measured ***E***-field intensity decreases radially in an exponential way at that position (not shown) is clearly an attribute of SWDs; such an exponential radial decay of the ***E***-field intensity was observed, according to Lebedev [6], along the plasma column up to approximately 90 mm, thus marking the end of the SWD. The first part of the curve up to 17 mm in Figure 3 is ascribed by Lebedev to space-wave radiation: as a matter of fact, when the electric antenna is axially set at 8 mm or at 90 and 110 mm from the launcher, the ***E***-field intensity radially decreases slowly away from the tube in contrast to the exponential radial decay observed within the SWD segment (corresponding figure in [6], not shown).

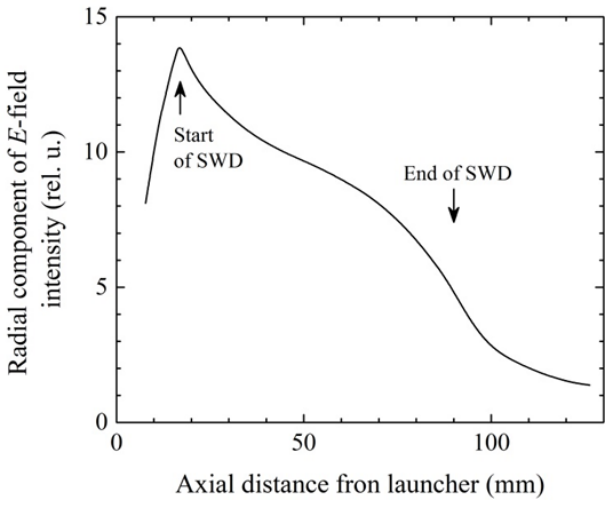

Figure 3: Radial component of the ***E***-field intensity detected with an electric antenna radially oriented with respect to the discharge tube as a function of axial distance from the launcher. The discharge is sustained in argon at atmospheric pressure from a Beenakker cavity supposedly operated on the TM_{010} mode at 2450 MHz (after [6]).

2.3 *Characteristics of the space-wave radiation region when sustaining a SWD with a surfaguide*

In the case of a surfatron, the interstice plane is perpendicular to the end of a coaxial (internal) transmission line terminated on its other end by a conducting reflecting wall [7], an arrangement that provides at the launching interstice an azimuthally symmetric power flow around the discharge tube. In

[3] In the near-field region of an antenna, the ***E*** and ***H*** field components are not yet necessarily perpendicular one to the other and in phase, which makes that the corresponding radiation is not that of (a true) EM wave.

contrast, the surfaguide wave-launcher [4] (Figure 4(a)) does not structurally ensure a similar azimuthally symmetric power flow at its exit around the discharge tube. This is because the movable plunger of the surfaguide system is tuned for maximum power transfer (minimum reflected power) to the plasma column, leading to a maximum of intensity of the standing wave (within the waveguide) that takes place essentially on the portion of the discharge tube wall facing the plunger: microwave irradiation of the cylindrical discharge tube is thus asymmetric, as clearly shown from numerical calculations (for instance [9]) and, for example, in Figure 4(b) at 210 μs.

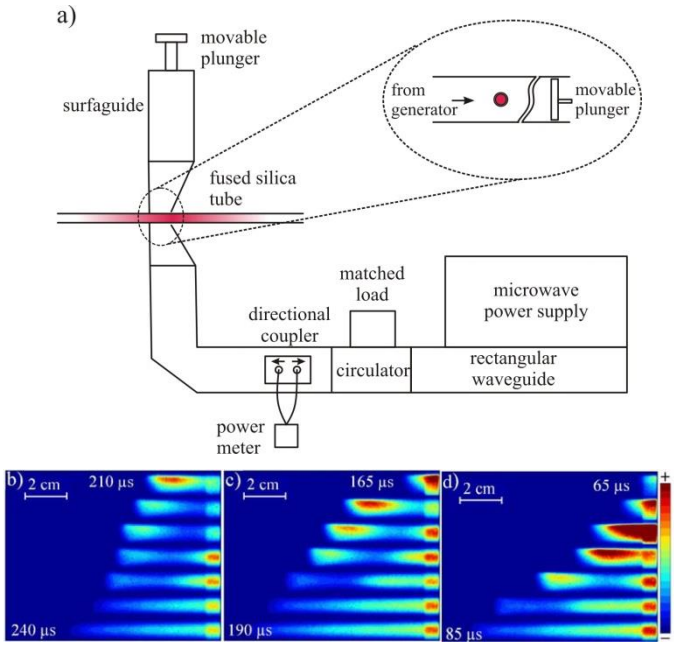

Figure 4: (a) Schematic diagram of the system utilized for achieving a SW plasma maintained with a surfaguide wave-launcher at 2450 MHz; (b), (c) and (d) are images taken with an iCCD under pulsed regime at a repetition rate of 50 Hz in helium gas at 5 Torrs (≈ 667 Pa) in a 8/10 id/od mm tube for 8, 16 and 23 W average absorbed powers, respectively, the plasma running from right (surfaguide interstice) to left on the pictures [1], [10].

Enlightening considerations characterising the space-wave radiation region can be obtained from a SWD sustained with a surfaguide and under pulsed regime operation, the mechanisms and properties of which are reported in [1]. Figures 4(b), 4(c) and 4(d) display the variation of the total emitted-light intensity at successive elapsed times (from top to bottom in the pictures), for a given average absorbed power. The plasma column runs from right (surfaguide interstice) to left on the pictures.

The maximum of light intensity observed in the initial moments of the discharge is gathered, on the photos, on the upper part of the discharge tube, i.e., on that sector of the tube wall facing the plunger (first upper row in (b), second upper row in (c) and third and fourth upper rows in (d)), which results, as already mentioned, from tuning for maximum absorbed microwave power with the movable plunger. Consider more specifically, for example, 210 μs in Figure 4(b): the light intensity of the discharge not being distributed symmetrically with respect to the tube axis indicates that a higher ionisation rate is occurring close to the wall situated on the plunger side; however, as time goes on, the plasma becomes azimuthally symmetric. In addition, after some elapsed time (at 225 μs in Figure 4(b) and earlier at higher average powers), a region of constant length and radial extent demarcates, in the end, as a small reddish rectangle (in the photo) in the immediate vicinity of the launching interstice (which we assign to the space-wave radiation region) while the plasma column develops in length with time (as a result of the propagation of the ionisation front of the SW initiating the SWD [1]). At the highest average power considered (Figure 4(d), 23 W), initially (≈ 68–75 μs) the plasma is non-azimuthally symmetric[5] over a longer plasma column length than at lower average powers. Nonetheless after some 75 μs in 4(d) and later on, the non-SWD plasma segment becomes constant in length (≈ 8 mm) and radial extent: these two features are then relevant to the space-wave radiation region reported under continuous operation (Figures 2(a) and 2(b)). Similarly, after a long enough on-time, the plasma column farther than the space-wave radiation region has become azimuthally symmetric, which we

[4] The gap of the launching interstice of the surfaguide is typically 15 mm wide for a WR-340 rectangular waveguide: it corresponds to the value of the tapering of the small wall of the waveguide such that the waveguide impedance matches that of the SW plasma column (seen as a transmission line). The thickness of the surfaguide plates forming the interstice is 0.9 mm [8].

[5] Close observation of this non-SWD region suggests that the EM field initially (and partially) progresses from the interstice along the upper wall of the dielectric tube, before it transforms into a SWD. In fact, a SW can propagate along a dielectric medium alone [11].

ascribe to a SW plasma column segment: it lends us to assume that the plasma column turns azimuthally symmetric at the same time that the propagating wave is a true EM wave, which it is not the case within the first part of the radiation zone (the near-field region of an antenna: see footnote 1). At this point, we conclude that the SWD develops once the radiation region has become constant in length and radial extent, and azimuthally symmetric.

From the various kinds of SWDs examined above, a general feature emerges: the extent in length of the space wave region decreases with frequency as reported in Table 1 (2450 MHz data for surfatron from [1], for surfaguide from [10]). The fact that the radiation segment extends on a distance much smaller than the wavelength, as reported in Table 1, is a characteristic of electromagnetically short antennas [12].

Table 1: Plasma column length of the space-wave radiation region L_{space} and ratio of L_{space} to corresponding EM wavelength in vacuum λ_0. Except otherwise indicated, there is no FC around the discharge tube.

Frequency (MHz)	Wave launcher	L_{space} (mm)	L_{space} / λ_0
360	Surfatron	330 ± 10	0.40
915	Surfatron	43 ± 1*	0.13
2450	Surfatron	28 ± 2	0.23
2450	Surfaguide	7 ± 1	0.06
2450	Beenakker Cavity	17	0.14

*With R_{FC} = 67.5 mm where cut-off radius ≤ 96.1 mm

The space-wave region becomes smaller and smaller as the applied field frequency is increased (in particular with the surfaguide as wave launcher).

2.4 *Minimum length of a Faraday cage (FC) at cut-off that significantly reduces perturbation to measurements due to space-wave radiation in the room*

Determining the characteristics of the SWD sustained at 915 MHz led us to abandon probing a plasma column completely open to free space: the radiation emitted by the space wave into the room prevents making reliable and reproducible measurements. We therefore turned to implementing coaxially to the discharge tube a cylindrical FC at cut-off immediately at the surfatron exit (see Figure 5), looking experimentally for the shortest such cage that would provide stable readings and recordings. A 30 mm long FC was found to do the job. This fact constitutes a further proof of the existence of a wave not guided along the plasma column (as a SW is), thus radiating into the room and that originates immediately past the launcher interstice showing, by the same token, that the SW, contrary to what was thought earlier, is not responsible for radiation in the room.

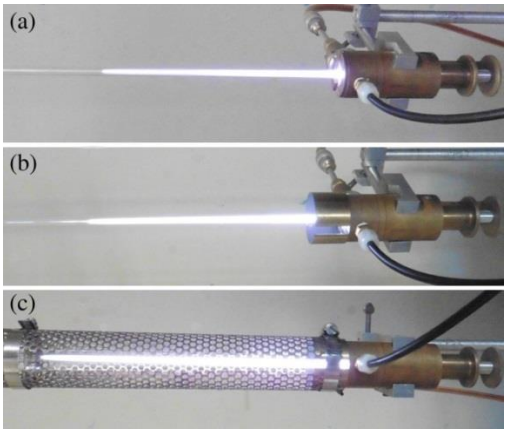

Figure 5: Photographs showing the plasma column obtained with a 915 MHz surfatron: a) no surrounding Faraday cage at all; b) enclosed in a 22.5 mm radius FC corresponding to wave cut-off in a circular waveguide (see footnote 2). The cage length is 30 mm, which was found to be the minimum FC length averting space-wave radiation from affecting much our measurements; c) enclosed in a 22.5 mm radius FC, 305 mm long, which is beyond the plasma column length. Absorbed power is 300 W in each photo. The axial slot in the FC allows making field intensity and spectroscopic measurements along the plasma column.

2.5 *Confining space-wave radiation increases the total amount of electrons in the discharge*

A possible way to cut down space-wave radiation losses is, as repeatedly indicated, to surround the discharge in a "circular waveguide" at cut-off. Such a FC prevents waves to propagate within it when bare: any radiation field entering the waveguide at cut-off gives rise to an evanescent field (exponential decay) with a zero Poynting vector in all directions. Nonetheless, propagation is possible within the waveguide enclosure when specific propagating structures are present: i) the SW propagates along the plasma column that it sustains in the case of SWDs

since it uses the dielectric discharge tube and the plasma contained as its propagating medium [1]; ii) a SW can also propagate along a dielectric tube, without depending on whether it contains some plasma or not. This is illustrated for an empty (no plasma) tube in Figure 3 of [1] where the wave propagation involves the whole circular part of the tube and, in Figure 4(b) (top picture) in the current paper, for that part of the dieletric tube wall facing the plunger close to which there is some plasma, the SW propagation around the tube being asymmetric.

Figures 6(a) and 6(b) display the axial distribution of electron density of the plasma column when enclosed inside a FC at cut-off: (a) with the FC of minimum length (30 mm); (b) with the longest FC (305 mm), longer than the plasma column at 915 MHz and 300 W. The data points are rather spread out in Figure 6(a), which results from the remaining space-wave radiation since the FC is only 30 mm long, in contrast to Figure 6(b) where the FC extends beyond the plasma column length.

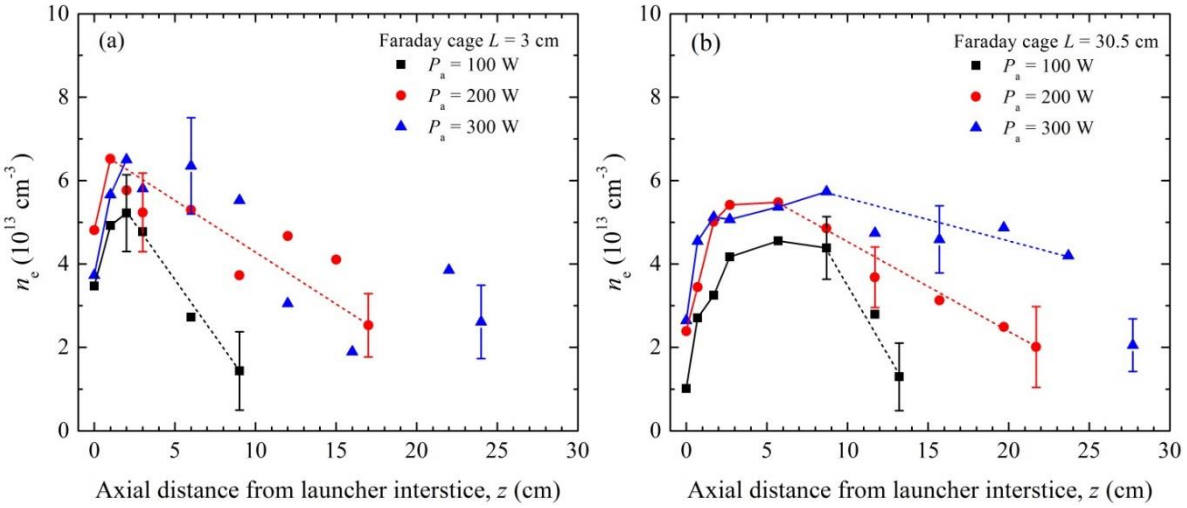

Figure 6: Axial distribution of electron density along a SWD sustained in argon at atmospheric pressure in a fused silica 6/8 mm id/od discharge tube and at 915 MHz, enclosed in a Faraday cage under cut-off conditions (R_{FC} = 22.5 mm): (a) minimum length FC (30 mm); (b) longest FC (305 mm), longer than the plasma column length at 300 W.

In Figure 6(a), the electron density increases as z increases from 0 up to 1 or 2 cm (space-wave radiation zone) and then decreases toward the end of the plasma column. At 100 W, this decrease is somehow linear, as expected when sustaining a SW plasma column; at 200 W, past the maximum of electron density, because of the error bars (due to radiation in the room), one can only suggest that the electron density decreases linearly. In contrast, in Figure 6(b), the maximum of electron density, reached at a higher z value (5 or even 7 cm), is not as sharp as in Figure 9(a) but extended, showing in fact what resembles a plateau, followed (within error bars) by a linear decrease of the electron density as expected from a SWD.

The electron density "plateau" noticed in Figure 6(b) contrasts with the expected linear decrease from a genuine SWD. We assume it to be related to the additional power flow carried by the SW propagating along the dielectric tube alone, as described three paragraphs above in (ii)). The existence of the plateau strongly suggests that there are two distinct power flows involved in the sustaining of the plasma column: otherwise, if the power flow carried by the dielectric tube alone had been merged with that of the SWD, it would have given a genuine SWD electron density linear decrease down the plasma column, starting at the electron density peak as in Figure 6(a).

Figures 7(a) and 7(b) show that the plasma length is significantly longer when the discharge tube is entirely surrounded by a FC at cut-off. At 915 MHz (Figure 7(a), obtaining a 250 mm long column requires less than 29% microwave power when inserted in the 305 mm long FC at cut-off when compared to its "minimum" 30 mm length. At 2450 MHz, although the extent of the space-wave region is shorter than at 915 MHz (Table 1), Figure 7(b) shows a similar power gain (or power saving): a 170 mm long plasma column, surprisingly, also requires

29% less power (the error bar in both figures is nonetheless ± 10%). The longer plasma column length obtained under cut-off conditions is the result of the SW power flow carried specifically along the dielectric tube (case ii) above). This additional contribution to electron density is further documented through Figure 8 below and examined in section 4.

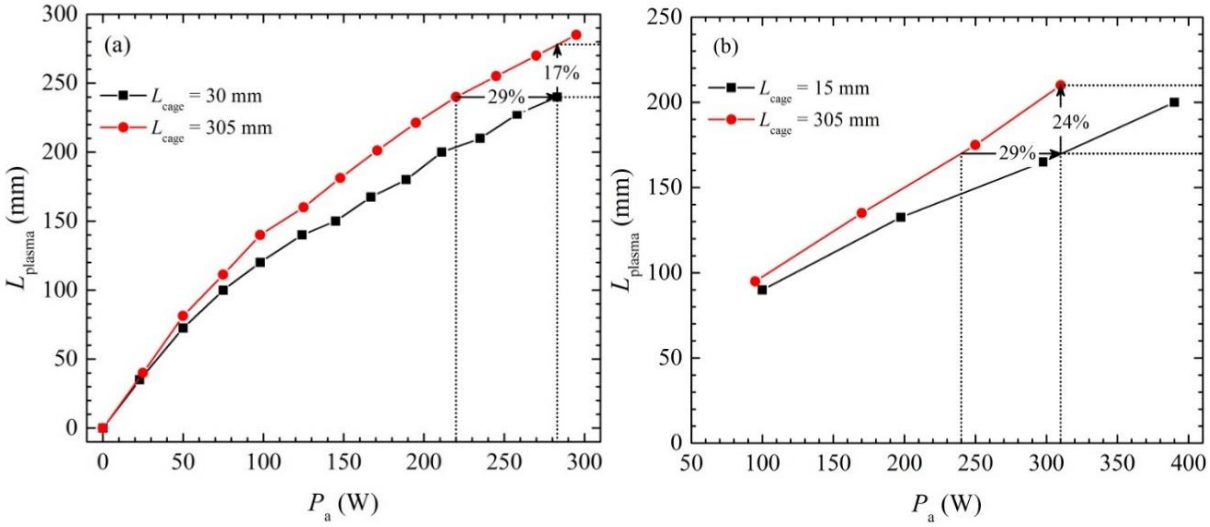

Figure 7: SWD column length as a function of microwave power when coaxially enclosed inside a cylindrical Faraday cage at cut-off (22.5 mm radius), one of minimum length (30 mm at 915 MHz in (a) and 15 mm at 2450 MHz in (b)) and the other being longer (305 mm) than the full length of the plasma column. At 915 MHz (a), 29% less power is required for a 240 mm long SWD fully surrounded by a FC at cut-off, while at 2450 MHz (b), also 29 % less power is needed for a 170 mm plasma length. The 915 MHz plasma column is sustained with a surfatron while at 2450 MHz the SWD is achieved with a surfaguide.

Figure 8 corresponds to the integration of the axial electron density distribution in Figures 6(a) and 6(b), obtained at 100, 200 and 300 W. Clearly, there are more electrons when the SWD is enclosed in a circular waveguide at cut-off; at 300 W, it means 30% more electrons, which is consistent with the power gain deducted from Figures 7(a) and (b).

Summarizing the findings of this section: i) space-wave radiation is, in a way, taking microwave power away from SWDs, the power being fully lost in the room when there is no FC at all; ii) the maximum increase in plasma length is obtained with a FC at cut-off that exceeds the plasma column length; iii) when the plasma column is completely enclosed in a FC, the microwave power absorbed per electron θ is clearly constant whatever the plasma column length (or microwave power). This comes out from the fact that, in Figure 8, the total average electron density (n_e total) increases linearly with microwave power, hence that the power absorbed per electron remains the same

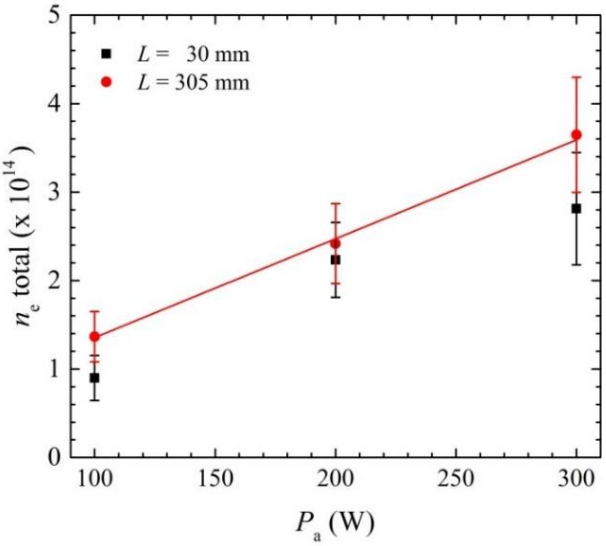

Figure 8: Average total electron density resulting from integration of the electron density axial distribution in Figures 6(a) and 6(b) at 915 MHz in argon gas at atmospheric pressure in a 6/8 mm id/od fused silica tube. The radius of the FC is 22.5 mm.

3 Calculated influence of the radius of a conducting enclosure on the SW plasma column length when not accounting for space wave radiation

When the radius of the metallic enclosure coaxially surrounding the SWD is sufficiently small, calculations predict a shorter plasma column than that observed experimentally. This comes out from Figure 9(a), which shows that for a 915 MHz ***E***-field, the length of the SW plasma column, initially without any conducting enclosure (R_{FC} > 1000 mm), first slightly increases when decreasing the cage radius, showing a longer plasma column at R_{FC} = 96.1 mm, which is the minimum radius of a FC achieving cut-off conditions; however, for smaller FC radii (now at cut-off), namely R_{FC} = 45 mm and 22.5 mm, the plasma column length becomes smaller and smaller: at R_{FC} = 22.5 mm, the plasma column is approximately half the length of that with no FC. This compelling outcome can be understood with Figure 9(b), which reveals (from right to left) that the attenuation coefficient α of the SW first decreases with decreasing FC radius, reaching a minimum value at approximately 130 mm: a smaller attenuation coefficient yields a lower electron density, hence a longer plasma column; afterwards, as R_{FC} keeps on decreasing, α increases, thus the plasma column length decreases. The end result in Figure 9(a) is in full opposition with experiments since, in reality, the SW plasma column becomes significantly longer when surrounded by a FC at cut-off (Figures 7(a) and (b)).

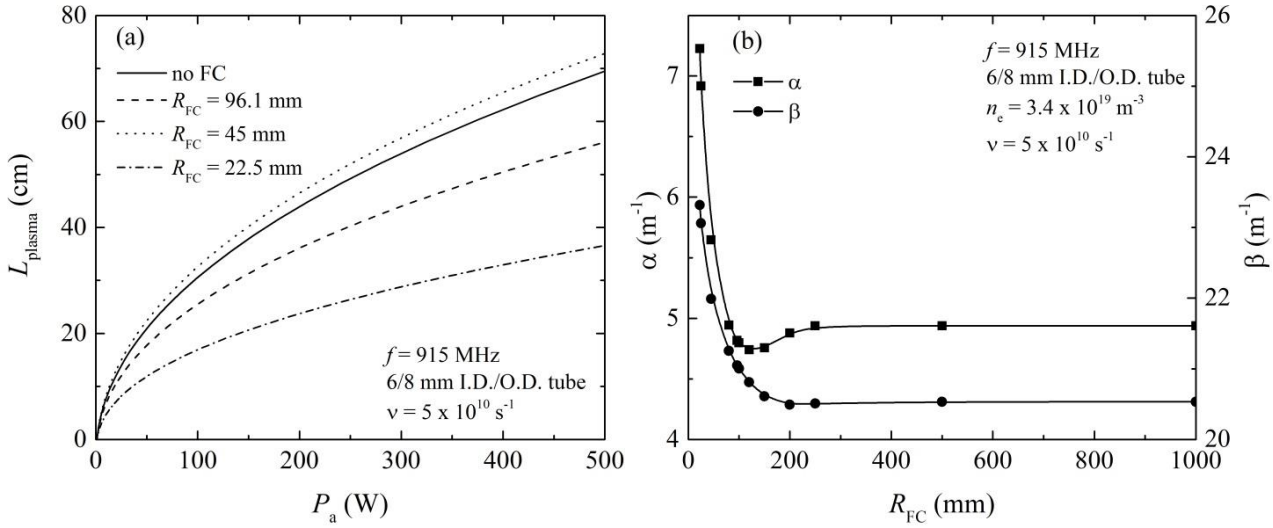

Figure 9: Ignoring the space-wave radiation phenomenon: (a) calculated plasma column length as a function of power in the following cases: open to free space (no FC), for the minimum R_{FC} ensuring cut-off (96.1 mm), and for R_{FC} = 45 mm and 22.5 mm (much below cut-off conditions); (b) calculated SW attenuation coefficient α showing that as a function of the FC radius it decreases drastically to reach a minimum value (130 $\pm$ 10 mm) and then slightly increases to set to a constant value.

4 Space-wave power loss as a function of the faraday cage (FC) length under cut-off conditions and corresponding radiation pattern

Figure 10 establishes through calculations (surfatron dimensions extended to 915 MHz from those of Hagelaar and Villeger at 2450 MHz [13]) and without any fitting that a little more than 30% of the power absorbed, originally intended to sustain the SW plasma column, is lost through space-wave radiation in the case of a discharge tube open to free space (no FC). As the FC length is increased up to 6 cm, the radiation power loss is found to drop off rapidly while for longer FC lengths, the power diminishes comparatively slowly to reach a zero value at L_{FC} = 22 cm, the assumed plasma column length for the calculations.

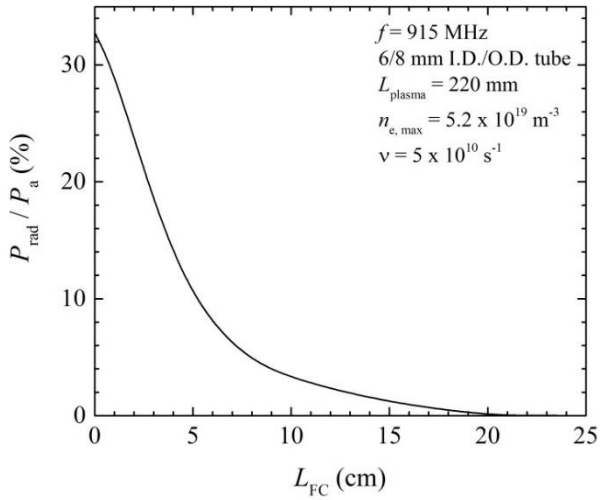

Figure 10: Calculated power radiated by the space wave as a function of the FC length at cut-off for a 2450 MHz surfatron wave launcher assumed operated at 915 MHz [13]. With no cage at all (L_{FC} = 0), approximately 30% of the absorbed power is lost in space-wave radiation. R_{FC} is presumed to be 22 mm and plasma column length 220 mm.

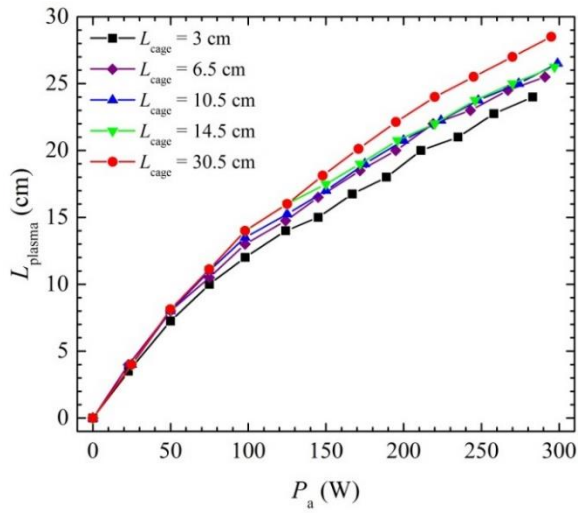

Figure 11: Measured plasma column lengths as functions of (absorbed) microwave power at 915 MHz for different lengths of the FC at cut-off. Same conditions as in Figure 7(a).

Figure 11 displays measured plasma column lengths as functions of microwave power at 915 MHz for different lengths of FC at cut-off (R_{FC} =22.5 mm). The shortest FC length examined is 3 cm, which is, as already mentioned, the minimum FC length under cut-off conditions ensuring stable and somehow reproducible measurements. Measured values obtained at 6.5 cm and up to 14.5 cm exhibit very similar plasma column lengths, as can be expected from calculations (Figure 10). The highest FC length considered, 30.5 cm, leads to a slightly higher plasma column length than the 6.5-14.5 cm set of curves. This is believed, as already mentioned, to be related to the fact that the FC then totally encloses the plasma column length, preventing wave reflection which occurs when part of the plasma column goes through the open end of a FC shorter than the plasma column itself.

Radiation pattern of the space wave

Figure 12 is the calculated radiation pattern for the EM space wave generated from a surfatron (behaving as an antenna) at 915 MHz and for different lengths of the FC at cut-off (R_{FC} = 22 mm). It shows a polar angle close to 30° when the discharge is open to free space while there appear two lobes with respect to approximately 0° when the FC length is 75 mm or longer, these lobes then becoming of lower and lower intensities, as expected from Figure 10.

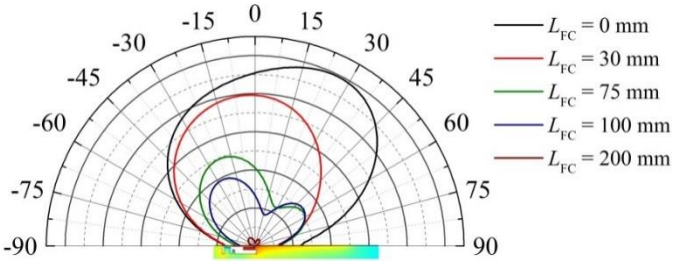

Figure 12: Calculated radiation pattern for the space wave in the case of a 915 MHz surfatron, as in Figure 13. The plasma column axis is aligned along the -90° – 90° line, which makes that the elevation angle Θ, determined with respect to the SW propagation direction (discharge tube axis), is thus complementary of the polar angle relatively to a right angle.

5 Discussion

High-frequency (HF) fields are present all along the plasma column even though the SWD is generated only at some distance away from the launcher. For the time being, the explanations that follow are mostly assumptions: i) the HF radiation coming out from the launching interstice is akin to the one encountered in the near-field region of (short) antennas [12], and within this region there should not be yet EM waves (no phase coherence between ***E*** and ***H***); ii) it is only at some distance past the near-field region that an EM field is constituted, which gives rise to space-wave radiation and, eventually, at the same location or near-by, to the EM SW that starts sustaining the plasma column; iii) in fact, the

maximum of HF field intensity reached (arrow in Figure 3) could mark the beginning of the formation of the true EM field. The question is whether the space wave and the plasma column SW are excited at this same location or the SW a little farther away down the plasma column; iv) when a FC at cut-off extends all along the plasma column length, the question is to what extent the space-wave radiation region has been reduced to the benefit of the SW propagating along the sole discharge tube, as discussed relatively to Figure 6(b).

6 Summary

To prove that a space-wave radiation segment necessarily anticipates the establishment of a SWD, three types of wave launcher, namely surfatron, surfaguide and Beenakker cavity, were utilized to that effect. In all three cases, it was observed that the SWD starts to develop only after the near-field radiation region, the axial length of which (above a minimum microwave power) does not increase with increasing power level, but its electron density as a whole does (Figure 2(a) and (b)). It was further observed that the length of this non-SWD plasma segment decreases when frequency is increased. To determine whether we were observing a SWD, we relied on the fact that the axial variation of electron density of SWDs, in contrast to the (initial) non-SWD segment, decreases linearly away from the launcher.

Non-guided radiating space waves had been first reported by Burykin et al [14] coming from a positive plasma column along which a (non-ionizing) SW had been launched. These authors attributed the far-field radiation pattern observed at an elevation angle $\Theta = 25°$ to a non-uniform portion of the cylindrical plasma column (a relatively abrupt change in the tube diameter) along which the SW was launched. Later on, space-wave radiation forerunning a SWD was disclosed by Lebedev [6].

We have shown that when sustaining a SWD, the accompanying space-wave generates EM emission in the lab with such intensity that it can prevent making reliable measurements. A relatively short length FC under cut-off conditions (30 mm and 17 mm long at 915 and 2450 MHz, respectively) is, in this case, enough to significantly reduce the non-guided wave radiation in the room. This constitutes a further confirmation of the existence of space-wave radiation. At the same time and in contrast, SWDs should no longer be held responsible for the high level of radiation observed in the room since the corresponding SW is well guided (and confined) along the plasma column.

Besides radiation in the environment, space-wave radiation is responsible for power losses, i.e., power not used to generate electrons in the SWD. For example, a FC under cut-off conditions with a length exceeding the SWD column length provides at 915 MHz in argon gas at atmospheric pressure 30% more electrons than with the 30 mm minimum length FC. In such a case, according to our assumption, the space wave is transformed into a SW using the dielectric tube (as if it were empty) as its propagating medium, providing additional power flow contributing to more electrons in the SWD, these two waves propagating independently.

7 Research perspectives

The power loss through space-wave radiation with its invasive emission in the environment is a negative aspect of using SWDs that should be dealt with. In particular, one should try to take advantage of the operating conditions (frequency, tube diameter, gas pressure). A possible application, provided the space-wave radiation issue can be brought to an acceptable level, is in replacing conventional fluorescent tubes (in particular no more mercury required).

Important open questions are: i) how is ionization achieved in the non-SWD segment; ii) where is the space-wave generated with respect to the SW sustaining the SWD; iii) how, when the plasma column is surrounded by a FC at cut-off, to describe the separate power flow of both SWs, specifically that propagating along the dielectric tube alone and that generating the SWD.

Acknowledgments

The authors wish to thank professors Ahmad Hamdan and John Michael Pearson together with Antoine Durocher-Jean, Ph.D. candidate, for commenting the manuscript and Dr. Danielle Kéroack for data processing, all from the Université de Montréal.

For further readings

1. M. Moisan, H. Nowakowska, *Plasma Sources Science & Technology* 2018, **27**, 073001.
2. V.M.M. Glaude, M. Moisan, R. Pantel, P. Leprince, J. Marec, Journal of Applied Physics 1980, 51, 5693-5698.
3. M. Moisan, R. Pantel, J. Hubert, *Contributions to Plasma Physics* 1990, **30**, 293-314.
4. H. Nowakowska, D. Czylkowski, Z. Zakrzewski, *Journal of Optoelectronics and Advanced Materials* 2005, **7**, 2427-2434.
5. Z. Zakrzewski, M. Moisan, G. Sauvé, Plasmas sustained within microwave circuits, in Microwave excited plasmas, M. Moisan and J. Pelletier, Editors. 1992, Elsevier: Amsterdam. p. 93-122.
6. Y.A. Lebedev, J. Moscow Phys. Soc. 1997, 7, 267-271.
7. M. Moisan, C. Beaudry, P. Leprince, *IEEE Transactions on Plasma Science* 1975, **3**, 55-59.
8. T. Fleisch, Y. Kabouzi, M. Moisan, J. Pollak, E. Castaños-Martínez, H. Nowakowska, Z. Zakrzewski, *Plasma Sources Science & Technology* 2007, **16**, 173-182.
9. H. Nowakowska, M. Jasiński, P.S. Dębicki, J. Mizeraczyk, *IEEE Transactions on Plasma Science* 2011, **39**, 1935-1942.
10. A. Hamdan, F. Valade, J. Margot, F. Vidal, J.P. Matte, *Plasma Sources Science and Technology* 2017, **26**, 015001.
11. F.J. Zucker, Surface-wave antennas and surface-wave-excited arrays, in Antenna engineering handbook, R.C. Johnson and H. Jasik, Editors. 1984, McGraw-Hill. p. 12.1-12.36.
12. C.A. Balanis, Antenna Theory: Analysis and Design. 2005: John Wiley & Sons, New Jersey.
13. G.J.M. Hagelaar, S. Villeger, *IEEE Transactions on Plasma Science 2005*, **33**, 496-497.
14. Y.I. Burykin, S.M. Levitskiy, V.G. Martynenko, *Radio Engineering and Electronic Physics* 1975, **20**, 86-91.

About the authors

Michel Moisan received the B. Sc. and M. Sc. degrees in Physics from the Université de Montréal and obtained a *Doctorat d'État (Docteur ès sciences)* from the Université Paris-XI in 1971. As his thesis work was an experimental demonstration of a Russian theory on High intensity EM field inducing periodic parametric instabilities in plasmas, he was invited by Academician L. A. Artsimovitch for a post-doctoral fellowship as a guest of the Soviet Union Academy of Sciences (Lebedev Institute, Moscow). He is currently *Professor emeritus* of the Université de Montréal. He received the *2017 Innovation award* from the European Physical Society (Plasma physics division) for various applications: industrial (abatement of greenhouse gases from microelectronics fabs, purification of krypton and xenon gases obtained from cryogenic distillation of air), medical (plasma sterilizer) and lab tools (surfatron, surfaguide and TIA/TIAGO wave-launchers to sustain highly reproducible plasmas). He is chevalier des *Palmes académiques* (République Française).

Pierre Levif received the M.S. degree in Biomechanics from the Université Paris-XII (Val-de-Marne, France) in 2003, the M.S. degree in Plasma physics from the Université Paris-XI (Orsay, France) in 2004 and the Ph.D in Plasma physics from the École Polytechnique (Palaiseau, France) in 2007. He was a physicist in the Groupe de Physique des Plasmas at the Université de Montréal from 2012 to 2018 where his interest focused mainly on the plasma sterilization of medical devices. Since 2013, he is also a Physics lecturer at the Université de Montréal.

Helena Nowakowska received the M.S. degree in physics from the Technical University of Gdańsk, Gdańsk, Poland, and the Ph.D. in ionized gases dynamics from the Szewalski Institute of Fluid-Flow Machinery, Polish Academy of Sciences, Gdańsk, Poland. Since 1985, she has been with Szewalski Institute of Fluid-Flow Machinery, Gdańsk, Poland, where she is currently a senior scientist. Her main interests include modeling of microwave discharges, designing microwave plasma sources and plasma kinetic processes.

High Current Pulsed ECR Ion Sources

V.A. Skalyga, S.V. Golubev, I.V. Izotov, R.L. Lapin, S.V. Razin, R.A. Shaposhnikov, A.V. Sidorov, A.V. Vodopyanov, A.F. Bokhanov, M.Yu. Kazakov

Federal Research Center "Institute of Applied Physics of the Russian Academy of Sciences"
46 Ul`yanova St., 603950 Nizhny Novgorod, Russian Federation
Contact Email: skalyga.vadim@gmail.com

Abstract

In present time some ECR ion sources use a high frequency powerful microwave radiation of modern gyrotrons for plasma heating. Due to high radiation power such systems mainly operate in a pulsed mode. This type of ECR ion sources was developed at the Institute of Applied Physics of Russian Academy of Sciences and the most part of experimental research was performed at SMIS 37 facility. At SMIS 37 gyrotrons with 37,5 and 75 GHz frequencies and 100 and 200 kW maximum power respectively are used for plasma production. Such heating microwaves allow creating plasma with unique parameters: electron density > 1013 cm-3, electron temperature 50-300 eV, ion temperature about 1 eV. The principal difference between these systems from the conventional ECR sources is a so-called quasi-gasdynamic regime of plasma confinement. In accordance with the confinement regime such sources have been called "gas-dynamic ECR sources". Typically, plasma lifetime in such systems is about 10 microseconds, which in combination with the high plasma density leads to formation of the plasma fluxes from a trap with density up to 1-10 A/cm2. The confinement parameter (the product of plasma density and lifetime) reaches a value (> 108 cm-3s) sufficient to generate multiply charged ions. The possibility of multiply charged ion beams (nitrogen, argon) production with currents up to 200 mA was demonstrated. Particularly the gas-dynamic ECR ion sources are effective for generation of high current proton beams with low emittance (high brightness). Recently a possibility of proton and deuteron beams formation with currents up to 500 mA and rms normalized emittance 0,07 pi • mm • mrad was demonstrated. The next step in the research is a transition to continuous wave (CW) operation. For this purpose, a new experimental facility is under construction at the IAP RAS. Future source will utilize 28 and 37,5 GHz gyrotron radiation for plasma heating. Overview of the obtained results and the status of the new source development will be presented.

1 Introduction

Production of high intensity ion beams from an ECR discharge could be realized in a pulsed mode when microwave power level coupled into a plasma is much higher than it is used in continuous wave (CW) operation. Basic principal is rather simple: a high current density ion beam could be produced in case of dense plasma flux from a magnetic trap coursed by fast losses; fast losses mean high heating power required for electron temperature sustaining at the level necessary for efficient ionization. Investigations of pulsed ECR discharge in an open magnetic trap under conditions of powerful ECR heating with gyrotron mm-waveband radiation were carried out over the last 20 years at the Institute of Applied Physics (IAP RAS, Nizhniy Novgorod, Russia) [1-5] and continued at Laboratoire de Physique Subatomique & Cosmologie (LPSC, Grenoble France) [6, 7]. In the beginning the work was devoted to development of a high frequency ECR source of multi-charged ions with outstanding parameters of plasma heating (37.5 GHz, 100 kW). According to Geller's scaling laws [8] such increase in frequency and power in comparison to conventional ECRIS was expected to boost the ion source performance and provide a significant progress in ECRIS development. However, due to short pulse operation mode and low repetition rate of the used gyrotrons (pulse duration < 1 ms, 0.1 Hz) breakdown and discharge conditions similar to a conventional ECRIS were unreachable. The minimum neutral gas pressure was two orders higher (10^{-4} mbar) and the plasma parameters differed significantly from conventional ECRIS. After years this work resulted in development of a new type of ion source – high current gasdynamic ion source.

2 Quasi-Gasdynamic Plasma Confinement

The use of powerful mm-band radiation allows to increase the plasma density in the discharge significantly (proportional to the square of the radiation frequency [4-9]) in comparison to conventional ECRISs, which utilize microwave radiation with frequencies on the order of 10 GHz [8]. In experiments with gyrotrons frequency range

37.5 – 75 GHz the plasma density reaches values of 10^{13} - 10^{14} cm^{-3}[10, 11]. Significant increase of the plasma density leads to a change of the confinement mode. A so-called quasi-gasdynamic confinement [4, 5] was realized in the presented experiments instead of the collision-less confinement [12], which is typical for modern ECRISs. The transition from collision-less to quasi-gasdynamic confinement occurs when the plasma density is high enough for the scattering rate of electrons into the loss-cone to be higher than the maximum possible electron loss rate caused by the ion-sound flux through the magnetic mirrors [13]. In such situation the loss-cone in the velocity space is populated, and the plasma lifetime does not depend on the collisional electron scattering rate into the loss-cone i.e. on the plasma density, but is determined by the trap size, magnetic field structure and ion sound velocity [13]. The plasma lifetime, which is much shorter than in conventional classical ECRISs, can be expressed as $\tau=(L\cdot R)/(2Vis)$, where L is the magnetic trap length, R the trap mirror ratio (ratio between magnetic field in the magnetic mirror and in the trap center) and Vis the ion sound velocity. Short plasma lifetime provides high plasma flux density from the trap. The flux is proportional to the plasma density and ion lifetime i.e. $I \sim N / \tau$, where N is the plasma density. Due to the high plasma density, the confinement parameter $Ne\cdot\tau$, which determines the ionization degree and average ion charge, can be as high as 10^8 – 10^9 $s\cdot cm^{-3}$, which is enough for efficient ionization. The main advantages of quasi-gasdynamic confinement are the following. The plasma lifetime does not depend on its density and, therefore increase of the density would lead to rising of confinement parameter and average ion charge. In addition, the plasma lifetime is proportional to the magnetic trap length and the source performance could be improved by adjusting the trap length. In case of extremely high frequency heating and accordingly higher plasma density multiple ionization is possible even in a small plasma volumes. ECR sources running under conditions of such plasma confinement are called gasdynamic ECRISs.

Possibilities and prospects of the gasdynamic confinement were demonstrated at SMIS 37 facility [4, 5] and at SEISM Prototype [6, 7]. It was shown that the described peculiarities of quasi-gasdynamic ECR discharge sustained by mm-waveband radiation, namely, short lifetime and high density, provide unprecedented ion current densities up to 800 emA/cm^2.

3 SMIS 37 Experimental Facility

The main part of the experiments devoted to the topic was conducted at SMIS 37 facility. During the years its configuration has been changing slightly, the latest one being schematically depicted in Fig. 1. The plasma is created and sustained inside a d=4 cm vacuum chamber (placed in a magnetic trap) by pulsed (1 ms) 37.5 GHz or 75 GHz linearly polarized gyrotron radiation with power up to 100 kW. The simple mirror magnetic field (or a cups trap for some experiments) is created by means of pulsed solenoids positioned at a distance of 15 cm from each other, providing a mirror ratio of 5. The magnetic field strength could be varied in a range of 1-4 T at mirror plugs, whereas the resonant field strength is 1.34 T for 37.5 GHz and 2.7 T for 75 GHz. The microwave radiation is coupled to the chamber quasi-optically through a quartz window and a special coupling system, which protects the window from the plasma flux. Quasi-optical coupling appears to be the best choice for high power microwave radiation transport into an ion source especially because air gaps additionally could be used as a DC-break between high voltage plasma chamber and microwave source. At SMIS 37 the pulsed gas feeding is used and gas line is incorporated into the coupling system i.e. the neutral gas is injected axially.

The ion extraction and beam formation is realized by a two-electrode (diode) system consisting of a plasma electrode and a puller. The diameter of the extraction aperture is varied from 1 to 10 mm. The distance between the extraction system and the magnetic plug at the center of the solenoid magnet was designed to be variable, which allows tuning the plasma flux density at the plasma electrode. The maximum applied extraction voltage is up to 100 kV. A Faraday cup with an aperture of 85 mm is placed right behind the puller (grounded hollow electrode) to capture the whole beam. The cup is equipped with an electrostatic secondary electron suppression. A 42° bending magnet is installed downstream in the beam line for measuring extracted beam spectrum.

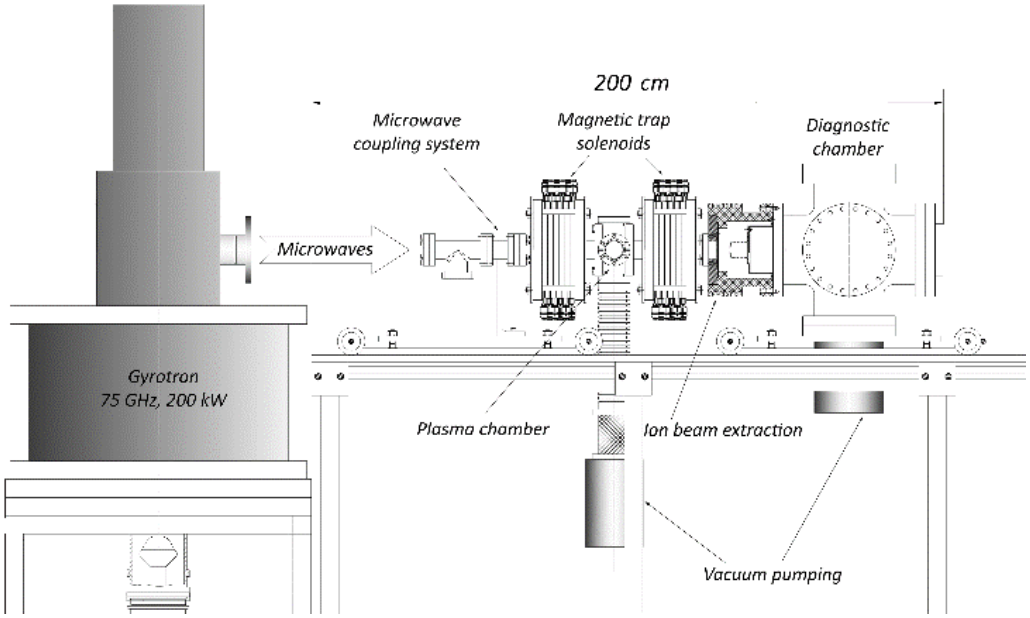

Figure 1: Schematic view of SMIS 37 experimental facility.

4 Multicharged Ions Production

A number of papers were devoted to multi-charged beam production at SMIS 37 [1-5]. In this paper the main results obtained some years ago are shown to demonstrate the typical source performance. In Fig. 2 two ion spectra with nitrogen and argon are presented in the case of 37.5 GHz, 100 kW plasma heating.

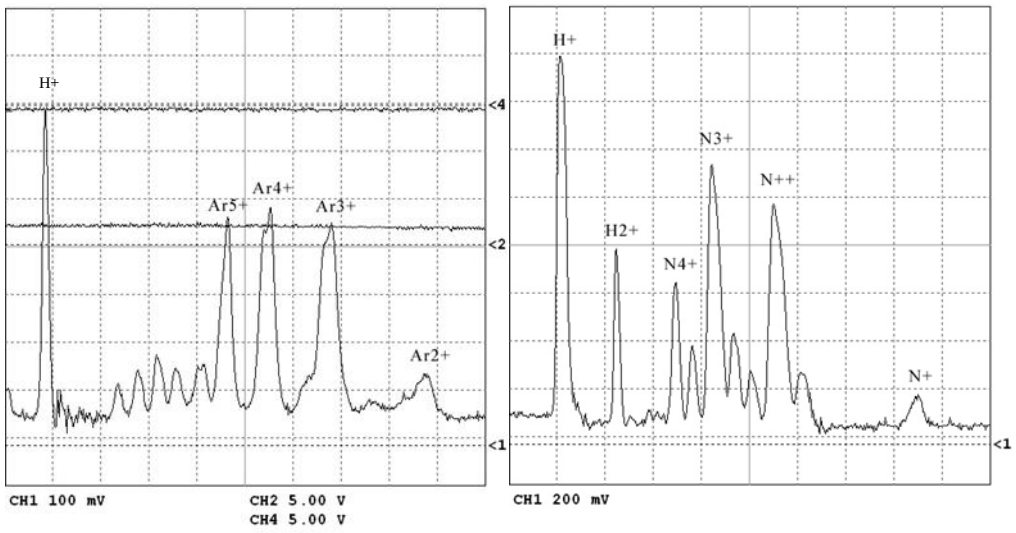

Figure 2: Argon and Nitrogen spectra. ECR plasma heating with 37.5 GHz, 100 kW gyrotron radiation in a simple mirror trap.

The effect of plasma density increase within gasdynamic confinement with increase of microwave frequency is shown in Fig. 3. Helium ion spectra for 37.5 and 75 GHz, 100 kW and 200 kW heating correspondingly demonstrate a great improvement in average ion charge.

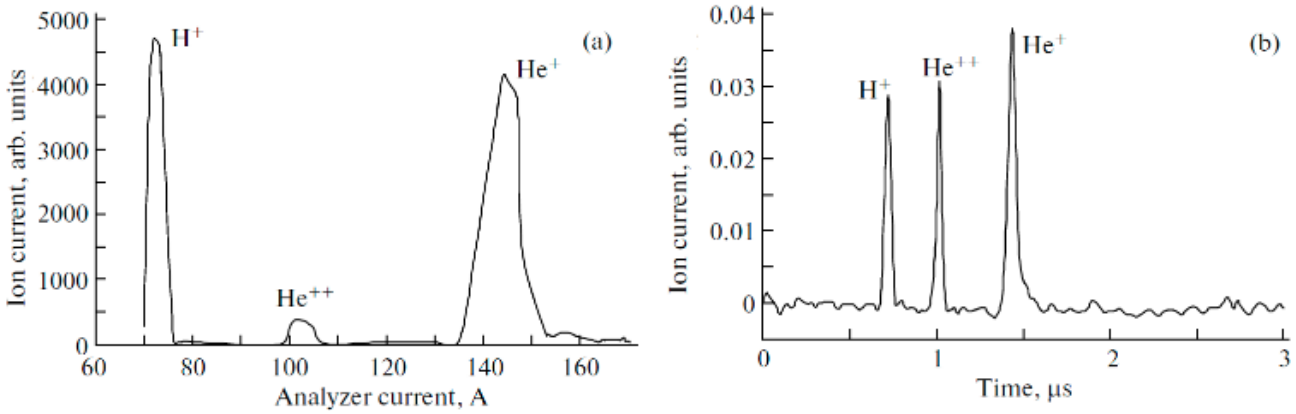

Figure 3: Helium spectra. 37.5, 100kW ECR heating (left) and 75 GHz, 200 kW ECR heating (right). Plasma is confined in a cusp trap with an effective length of 28 cm, the gas pressure is 10^{-4} Torr.

In these experiments a single aperture two electrode extraction system with 1 mm hole was used for beam formation providing total ion current up to 10 mA [2]. Normalized beam emittance measured with pepper-pot method was of the order of 0.01 π·mm·mrad. The experiments were repeated later with multi-aperture extraction systems. Extracted ion current dependence on the accelerating voltage in case of 13-hole (each 3 mm in diameter) plasma electrode is shown in Fig. 4.

Presented results demonstrate that gasdynamic ion source is able to produce hundreds of emA of moderately charged (Q up to 6+) beams. Low emittance and high current of such beams may allow using them together with charge-breeding or stripping techniques. Further increase of the microwave frequency is promising for the production of high current heavy ion beams with the average charge about +10 and their injection into accelerators with strippers after first acceleration stage.

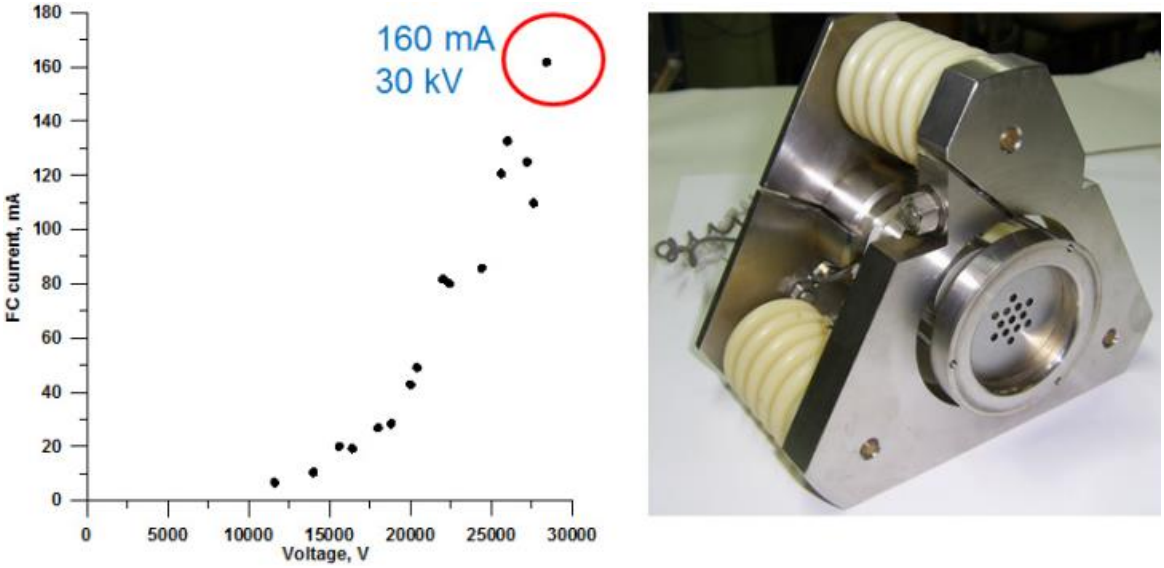

Figure 4: Faraday cup current dependence on extraction voltage (left) obtained with multi-aperture extraction system (right)

.

The state of the art ion source of this type called SEISM Prototype have been built recently in Grenoble in frames of international collaboration between LPSC, IAP RAS and LNCMI (CNRS). It is the first ECRIS with a topologically closed 60 GHz ECR resonance zone, using radially cooled polyhelices. Unique ion beam intensities have been extracted from this prototype, like 1.1 mA of O^{3+} through a 1mm hole representing a current density of 140 mA/cm^2 [7]. In first experiments a significant

current of highly charged ions like O^{5+} were also observed. Further investigation at this experimental facility should demonstrate the ultimate performance of gas dynamic ECR ion sources.

5 Short Pulse Ion Beams

Many of the modern technologies and basic research facilities require the creation of an ion source capable of generating short-pulse (20 – 100 μs), high current (tens or hundreds of milliamps) heavy gases ion beams with a fairly high average charge and low emittance. Gasdynamic ECR sources of multicharged ions seem to be the most promising in this respect. In this case, the plasma confinement in a magnetic trap is quasigasdynamic and has a typical lifetime of 10 to 20 μs. Under these conditions, there are two modes of generating high-current ion pulses of short duration, namely, quasi-stationary and non-stationary. The possibility of quasi-stationary generation of short-pulse multicharged ion beams is related to a short plasma lifetime in the trap of a gas-dynamic ECR source, which ensures that the plasma density can reach a steady-state level within a short time. To obtain short pulses in the non-stationary generation mode, one can use the well-known preglow effect [14 - 17], in which a peak current of extracted multiply charged ion beam with amplitude exceeding several steady-state values is observed at the initial stage of a discharge. In addition, it was found in [18] that in the case the gyrotron pulse duration is less than or of the order of the typical time of the preglow peak formation the beam current occurs predominantly after the end of the microwave pumping in the form of an intense short burst. Apparently a similar effect was observed earlier in [19] and was named "the micropulsed mode". In experiments conducted at SMIS 37 it was demonstrated that gasdynamic ECR ion source running in such "micropulsed mode" is able to produce multicharged ion beams with duration less than 100 μs. Waveforms of the full beam current and for Ar^{4+} and Ar^{5+} currents are shown in Fig.5.

The total beam current extracted with multi-aperture extraction system described above was at the level of 100 mA.

Later some theoretical work showing a possibility of high ionization efficiency in case of short-living radioactive isotopes beams production was reported in [20]. For the needs of Beta Beam project [21] it was shown that gasdynamic ECR source in the short pulse mode could provide up to 50% utilization of ^{6}He in fully striped ion.

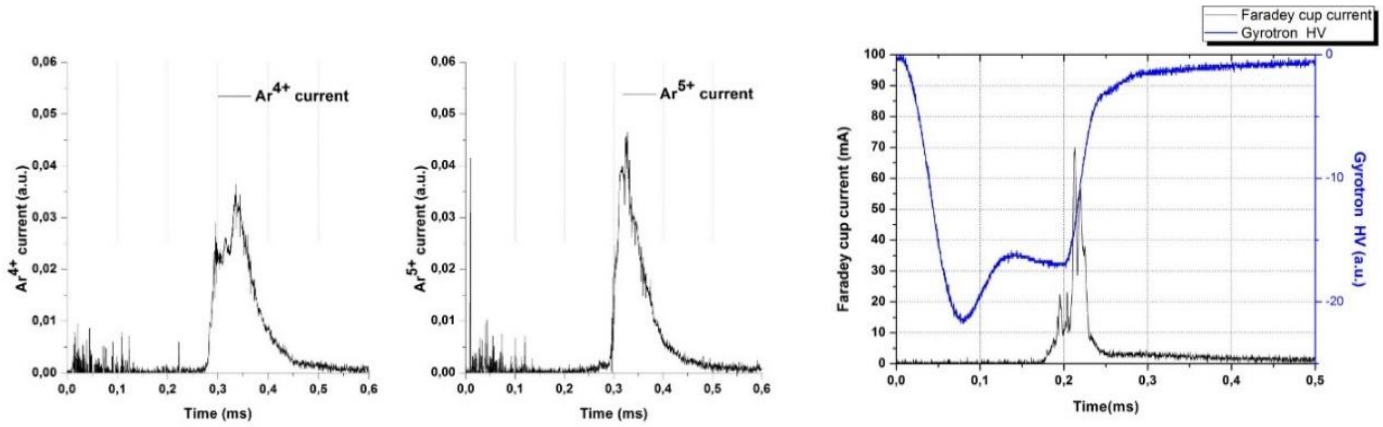

Figure 5: Oscillogram of the argon ion beam current (Faraday cup current) for an extraction voltage of 23 kV is on the left. High-voltage pulse of the gyrotron cathode (which duration is close to the one of microwave power pulse) is shown. Corresponding currents of separate beam species (Ar^{4+} and Ar^{5+}) are on the right.

6 Proton and Deuteron Beams Formation

Operation of modern high power accelerators often requires production of intense proton and deuterium beams. H+ beams are utilized or envisioned for use in linear accelerators e.g. the future European Spallation Source under design [22, 23]; some special applications such as neutron generators or the IFMIF project, require D+ (deuteron) ion beams. Requirements for the brightness of such beams grow together with the demand of accelerator development

and arising experimental needs. New facilities aiming at outperforming the previous generation accelerators are usually designed for higher beam currents. Enhancing the beam intensity and maintaining low transverse emittance at the same time is, however, quite a challenging task. The most modern accelerators require H+/D+ ion beams with currents up to hundreds of emA (pulsed or CW), and normalized emittance less than 0.2 π·mm·mrad [22, 24] to keep the beam losses at high energy sections of the linacs below commonly imposed 1 W/m limit. Previous experiments on heavy multi-charged ion production demonstrated that gasdynamic ion source is able to produce ion beams with record beam current density and moderate ion charge. The average electron energy in plasma of ECR discharge with quasi-gasdynamic confinement sustained by gyrotron radiation varies from 50 to 300 eV and it is optimal for efficient hydrogen ionization. Due to this coincidence it was decided to test the gasdynamic ECR source performance for proton and deuteron beams formation. In previous papers [25, 26] it was demonstrated that proton beams with current of hundreds of mA could be produced. The latest results are presented below.

A single-aperture extraction system was used for beam formation in the presented experiments. As only two fixed puller holes were available (i.e. 10 and 22 mm in diameter), the optimization of extraction electrode configuration was done varying the gap between the electrodes The biggest hole diameter in plasma electrode was 10 mm. In this case the optimal gap between electrodes for 10 mm plasma electrode aperture appeared to be 6 mm, while the puller hole diameter was 22 mm. The Faraday cup and puller currents are shown in Fig. 6(a). The total beam current remains relatively stable at the level of 450 mA through 70% of the microwave pulse. Accelerating voltage of 41.5 kV was used. Transversal emittance diagram is presented in Fig. 6(b), showing an RMS value of 0.07 π•mm•mrad.

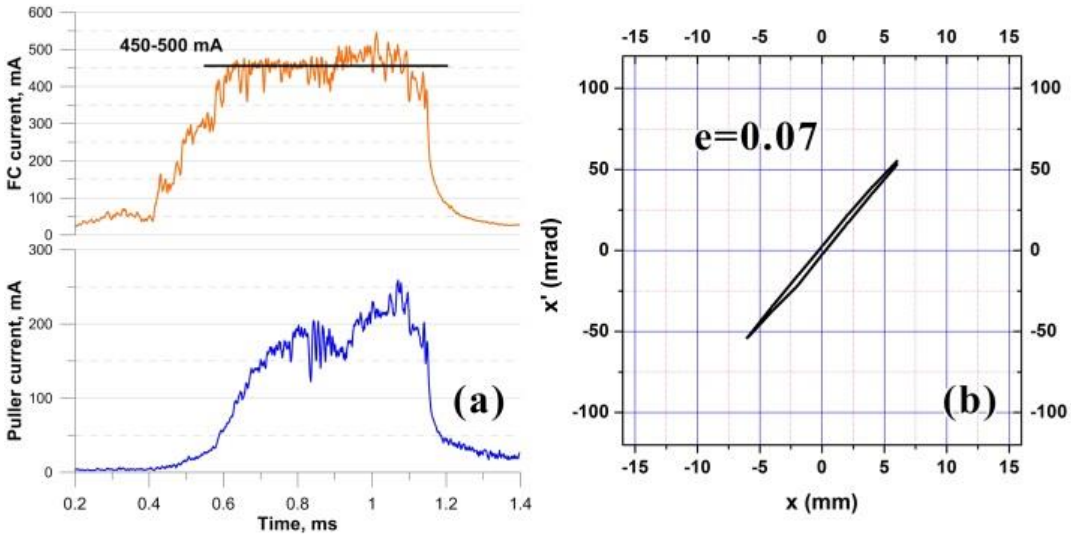

Figure 6: Hydrogen, 10 mm plasma electrode hole (a) Faraday cup and puller currents, (b) RMS emittance diagram.

The experiments with deuterium were performed under similar conditions. Source settings were adjusted slightly from the optimal ones for proton beam to maximize the total current. It was observed that the total beam current rapidly reached a value of 400 mA, then slowly increased to 500 mA and remain there till the end of the microwave pulse. Accelerating voltage of 42 kV was used. Transversal emittance had the same RMS value of 0.07 π·mm·mrad.

The presented results demonstrate the prospects of the high current gasdynamic ECR source for light ion beams production. The maximum RMS brightness of extracted beam reached 100 $A/(\pi \cdot mm \cdot mrad)^2$. The proton (deuteron) fraction in extracted beams was about 94 % as it was shown in [25].

The extracted beam current could be further enhanced by moving the plasma electrode closer to the magnetic mirror and scaling the extraction

voltage and geometry appropriately. According to simulations, the extracted current may eventually exceed 1 A while maintaining the low emittance. Such result would outperform the conventional ECRISs by a great margin.

7 Continuous Wave Operational "GISMO" Experimental Facility

The main part of previous experiments was carried out in a pulsed operation mode. Preliminary studies of plasma parameters were performed using a CW source with 24 GHz/5 kW gyrotron heating [27]. Obtained experimental results have demonstrated that all gasdynamic source advantages could be realized in CW operation. To continue development of a CW gasdynamic ion source a new experimental facility named GISMO (Gasdynamic Ion Source for Multipurpose Operation) is under construction at the IAP RAS. Future facility have been named GISMO (Gasdynamic Ion Source for Multipurpose Operation). This facility is aimed to produce continuous high-current (>200 mA) ion beams with low emittance (<0.2 π·mm·mrad). The scheme of the future experimental facility is show in Figure 7. The key elements of the setup are 28 GHz/10 kW and 37,5 GHz/20 kW CW gyrotrons manufactured by Gycom [28]. These microwave generators are equipped with power supplies suitable for CW or pulsed operation. A fully permanent magnet magnetic trap is used for plasma confinement. Magnetic field configuration was designed to be similar to a simple mirror trap close to the system axis with field strength at magnetic mirrors of 1.5 T and mirror ratio close to 6. Distance between magnetic mirrors is about 12 cm. For ion beam extraction it is planned to use 3 or 4-electrode system with maximum acceleration voltage up to 100 kV. Such extraction requires development of an appropriate high-voltage insulation of the discharge chamber from other parts. In this regard, one of the key elements of the installation is the DC-break of the microwave transmission line. It was proposed to implement a quasioptical system shown in Fig. 7.

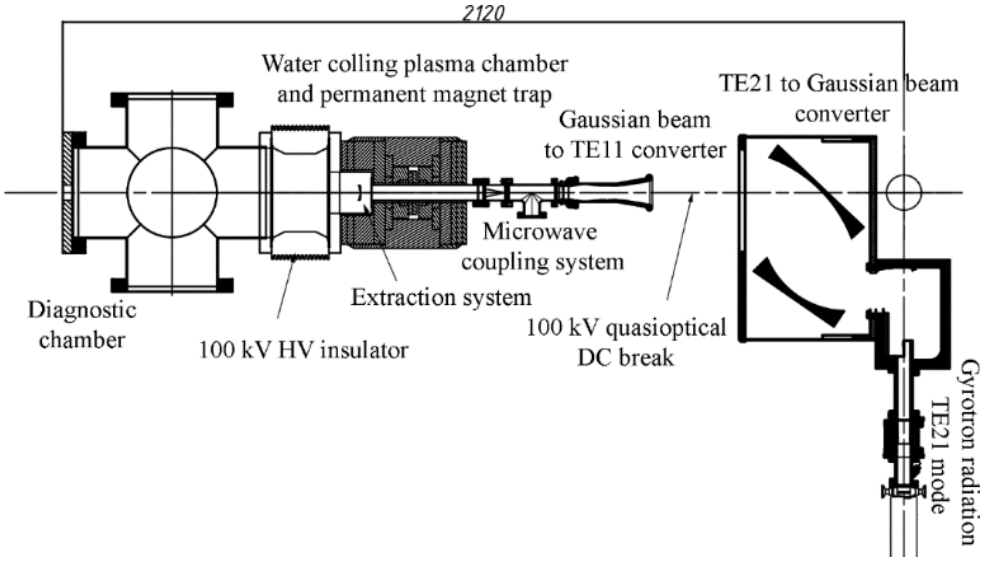

Figure 7: Scheme of the GISMO 28/37 CW high current ion source.

Plasma chamber is 30 cm in length and 4 cm in diameter. It is equipped with water cooling along whole surface from the coupling system to the flange.

First results at GISMO facility would be published at the end of the year 2018.

8 Conclusion

The presented results demonstrate the main prospects of the gasdynamic ECRIS. This type of ECRIS has already demonstrated its benefits for light ion beam production. Further studies could significantly increase its performance in multi-charged beam formation. One of the most promising new ion sources which may demonstrate all

capabilities of gasdynamic confinement is the SEISM, 60 GHz ECRIS at LPSC, Grenoble. The Grenoble facility has a number of advantages in comparison with SMIS 37. The first is a high repetition rate (up to 2 Hz) which allows better control of plasma parameters due to satisfactory wall conditioning. The second is the cusp magnetic field of high intensity (up to 7 T) with closed ECR surface. It is the first ion source which can operate effectively in gasdynamic mode having a closed-ECR field, which is of great importance for trapping of energetic electrons. Therefore, interesting results are foreseen from SEISM source, as it may be the first ECRIS able to operate in-between of gasdynamic and traditional collision-less confinement, thus producing high currents and charges.

Acknowledgments

The work is being realized in frames of realization of Federal targeted program R&D in Priority Fields of the S&T Complex of Russia (2014-2020) contract #14.604.21.0195 (unique identification number RFMEFI60417X0195).

For further readings

1. S.V Golubev, S.V. Razin, A.V. Sidorov, V.A. Skalyga, A.V. Vodopyanov, V.G. Zorin, "High Current Density Ion Beam Formation from Plasma of ECR Discharge", *Review of Scientific Instruments*. 2004, **75 (5)**, 1675-1677.
2. S.V. Golubev, I.V. Izotov, S.V. Razin, V.A. Skalyga, A.V. Vodopyanov, V.G. Zorin. Multicharged Ion Generation in Plasma Created by Millimeter Waves and Confined in a CUSP Magnetic Trap. *Transactions of Fusion Science and Technology*, 2005, **47 (1T)**, 345-347.
3. A. Sidorov, I. Izotov, S. Razin, V.Skalyga, V. Zorin, A. Balabaev, S. Kondrashev, A Bokhanov. Beam Formation from Dense Plasma of ECR Discharge. *Review of Scientific Instruments*., 2006, **77(3)**, 03A341-1 – 03A341-4.
4. V. Skalyga, V. Zorin, I. Izotov, S. Razin, A. Sidorov, A. Bohanov. Gasdynamic ECR Source of Multicharged Ions Based on a Cusp Magnetic Trap. *Plasma Sources Science and Technology*, 2006, **15,** 727-734.
5. S. Golubev, I. Izotov, S. Razin, A. Sidorov, V. Skalyga, A. Vodopyanov, V. Zorin, A. Bokhanov. High Current ECR Source of Multicharged Ion Beams. *Nuclear Instruments and Methods in Physics Research B*, 2007, **256**, 537 – 542.
6. M. Marie-Jeanne et al., "Status of the SEISM experiment", proceedings of the 20th International Workshop on Electron Cyclotron Resonance Ion Sources ECRIS2012, Sydney, Australia, pp. 111-113,
7. Lamy, T. et al Proceedings of the 13th International Conference on Heavy Ion Accelerator Technology. P. THM2I01.
8. Geller R. Electron cyclotron resonance ion sources and ECR plasmas. Institute of Physics. Bristol. 1996.
9. M.A. Dorf, V.G. Zorin, A.V. Sidorov, A.F. Bokhanov, I.V. Izotov, S.V. Razin, V.A. Skalyga. Generation of Multi-Charged High Current Ion Beams using the SMIS 37 Gas-dynamic Electron Cyclotron Resonance (ECR) Ion Source. *Nuclear Instruments and Methods in Physics Research (section A: Accelerators, Spectrometers, Detectors and Associated Equipment)*, 2014, **733**, 107-111.
10. Golubev S V et al 2000 *Rev. Sci. Instrum*., 2000, **71(2-2)**, 669.
11. Vodopyanov A V et al 2007 High Energy Phys. and Nucl. Phys. 31(S1), 152
12. Pastukhov V *Voprosy teorii plasma*, 1984, **13**, 160.
13. Mirnov V.V., Ryutov D.D., *Pisma v Zhurnal Theknicheskoi Fiziki*, 1979, **5,** 678
14. V.G. Zorin, V.A. Skalyga, I.V. Izotov, S.V. Razin, A.V. Sidorov, T. Lamy, T. Thuillier, *Trans. Fusion Sci. Technol.*, 2011, **59**, 140.
15. T. Thuillier, T. Lamy, L. Latrasse, I.V. Izotov, A.V. Sidorov, V.A. Skalyga, V.G. Zorin, M. Marie-Jeanne, *Rev. Sci. Instrum.* 2008, **79**, 02A314.
16. I.V. Izotov, A.V. Sidorov, V.A. Skalyga, V.G. Zorin, T. Lamy, L. Latrasse, T. Thuillier, *IEEE Trans. Plasma Sci.* , 2008, **36**, 1494.
17. V. Skalyga, I. Izotov, V. Zorin, and A. Sidorov. Physical principles of the preglow effect and scaling of its basic parameters for electron cyclotron resonance sources of multicharged ions. *Physics of Plasmas*, 2012, **19**, 023509.
18. V. Skalyga, I. Izotov, S. Razin, A. Sidorov, V. Zorin, Proceedings of the 8-th International workshop «Strong microwaves and terahertz waves: sources and applications». Nizhny Novgorod - St. Petersburg, Russia, July 9-16, 2011, p. 200-201.
19. L. Maunoury, L. Adoui, J.P. Grandin, F. Noury, B.A. Huber, E. Lamour, C. Prigent, J.P. Rozet, D. Vernhet, P. Leherissier, J.Y. Pacquet, *Rev. Sci. Instrum*. 2008, **79**, 02A313.
20. I. V. Izotov, V. A. Skalyga, V. G. Zorin. Optimization of gas utilization efficiency for short-pulsed electron cyclotron resonance ion source. *Rev. Sci. Instrum.*, 2012, **83**, 02A342.
21. beta-beam.web.cern.ch
22. Gammino S et al, LINAC2010, Tsukuba, Japan, THP116, (2010). http://www.JACoW.org
23. Lindroos M et al., *Nucl. Instrum. Methods B*, 2011, **269**, 3258.
24. Gobin R et all, *Rev. Sci. Instrum.*, 2012, **83**, 02A345
25. V. Skalyga, I. Izotov, S. Razin, A. Sidorov, S. Golubev, T. Kalvas, H. Koivisto, and O. Tarvainen. "High current proton beams production at Simple Mirror Ion Source 37". *Review of Scientific Instruments*, 2014, **85(2)**, 02A702-1 – 02A702-3.

26. 25) V. Skalyga, I. Izotov, A. Sidorov, S. Razin, V. Zorin, O. Tarvainen, H. Koivisto, T. Kalvas. High current proton source based on ECR discharge sustained by 37.5 GHz gyrotron radiation. *JINST*, 2012, **7**, P10010.
27. Skalyga, V., Izotov, I., Golubev, S., Vodopyanov, A., & Tarvainen, O., First experiments with gasdynamic ion source in CW mode. *Review of Scientific Instruments*, 2016, **87(2)**, 02A715.
28. www.gycom.ru

About the author

Skalyga Vadim was born in 1981 in Gorky, USSR (now Nizhny Novgorod, Russia). In 2004 he graduated from the Faculty of Higher School of General and Applied Physics of the Nizhny Novgorod State University, receiving a master's degree in physics with honors. Since 2001 he has been working in the Department of Plasma Physics and High Power Electronics of the Institute of Applied Physics of Russian Academy of Sciences, first as a senior laboratory assistant researcher, from 2004 to 2007 - as a junior researcher, from 2007 to 2010 as a researcher, from 2010 to 2013 - as a senior researcher, from 2014 to the present, as the head of the Ion Sources Laboratory. In 2007 he defended PhD thesis “Study of ECR sources of multiply charged ions with quasigasdynamic plasma confinement in open magnetic traps” in the field of physical and mathematical sciences with “plasma physics” specialization. In 2017 he successfully defended his thesis for Doctor of Sciences degree named “Study of an electron cyclotron resonant discharge for production of intense ion beams”.

industry engagement and consultancy at SCAN, Duan has developed broader experience with materials analysis and investigation in the areas of construction, manufacturing, preservation and environmental science. His experience with interdisciplinary projects has given him expertise with understanding and comparing the advantages and disadvantages of a suite of analytical techniques including gas chromatography mass spectrometry (GCMS). He currently manages Trace Analysis for Chemical, Earth and Environmental Sciences (TrACEES) platform in aim to develop advanced analytical capabilities and capacities for multidisciplinary researches and technical supports.

Highlight of the 10th International Workshop on Microwave Discharges: Fundamentals and Applications (MD-10) 3-7 September, 2018, Zvenigorod, RUSSIA

Yuri A. Lebedev

Head of Laboratory of Plasma Chemistry and Physical Chemistry of Pulse processes,
Topchiev Institute of Petrochemical Synthesis RAS (Moscow, Russia)
Contact Email: lebedev@ips.ac.ru

International Workshop "Microwave Discharges: Fundamentals and Applications" is a three-year periodical meeting which is held by turns in Russia and out of it. The main purpose is to discuss recent achievements in the study of microwave plasma, to identify directions for future research, and to promote close relationship between scientists from different countries. Activity of the Workshop is controlled by the International Scientific Committee.

Members of ISC in 2018 were: J. Asmussen (USA), P. Awakowicz (Germany), E. Benova (Bulgaria), F. Dias (Portugal), A. Gamero (Spain), E. Jerby (Israel), Yu. Lebedev (Russia, Chairman), A. Lacoste (France), M. Moisan (Canada), M. Nagatsu (Japan) J.J.A.M. van der Mullen (Belgium). Honorary Members of ISC: M. Kando (Japan), J. Marec (France).

Information support: Association for Microwave Power in Europe for Research and Education (AMPERE), Scientific and Technical Journal “Prikladnaya Fizika” (Applied Physics).

Calendar of the International Workshops: Portugal (1992), Russia (1994), France (1997), Russia (2000), Germany (2003), Russia (2006), Japan (2009), Russia (2012), Spain (2015), Russia (2018).

MD-10 took place in the town Zvenigorod (Russia) in the Rest Home of the Russian Academy of Sciences (Fig. 1) located 50 km to the North-West of Moscow in a picturesque place of the Moscow region close to Zvenigorod town (Fig. 2). This region is known as "Russian Switzerland".

Organizers: European Physical Society**,** Russian Foundation for Basic Research**,** Russian Academy of Sciences**,** The United Physical Society of the Russia, Scientific Council of RAS on Physics of Low temperature plasma**,** Scientific Council of RAS on Plasma Physics**,** Topchiev Institute of Petrochemical Synthesis of the Russian Academy of Sciences**,** Prokhorov General Physics Institute of the Russian Academy of Sciences**,** Science and Technology Center PLASMAIOFAN.

Figure 1: Photograph of participants at the entrance of the Rest Home.

Figure 2: Moskva-river near Zvenigorod upstream from Moscow

The Workshop was opened on the morning of September 3 and before the start of the scientific program the Chairman of the Workshop Prof. Yu.A. Lebedev congratulated the member of the ISC Prof. M. Moisan (Fig. 3) on two events. They are the high title of Chevalier dans l'Ordre des palmes académiques of the French Republic and Innovation Award of the European Physical Society "For pioneering contributions to the development and understanding of microwave plasma sources and their application to material processing, healthcare and environmental protection"**.**

Figure 3: Chairman of the first session and member of ISC Prof. M. Moisan

Figure 4: View from the roof of the Rest Home

All topics of microwave plasma theory and generation, microwave plasma diagnostics, modeling and application were presented in 12 plenary, 10 invited, 10 topical and 14 poster presentations. Most of plenary lectures were presented by young scientists. The scientific program was built without parallel sections so that all participants could discuss all the reports. This principle of the Workshop is laid down in its Constitution. 44 attendants came from 15 countries (Belarus, Belgium, Canada, Czech Republic, Germany, Greece, Japan, France, Korea, Israel, Bulgaria, The Netherlands, Portugal, and Russia). A coffee breaks took place on the roof of the Rest Home, from where a beautiful view of the surroundings was opened (Fig. 4). The weather was excellent and the poster session also was held on the roof of Rest Home.

Welcome party with a fire (Fig.5) was held in a clearing in the forest near the house near the fire. Despite the inclement weather, everything went very well.

Figure 5: Welcome fire

Figure 6: The Arbat street.

The social program of the Workshop included bus and walking tour on Moscow. Participants

visited the pedestrian Arbat Street, where artists present their paintings (Fig.6).

Then they went to the Theater Square where the Bolshoi Theater is located and went to Red Square (Fig.7). The following was a visit to the Tretyakov Gallery of Art, where paintings of outstanding Russian artists of different times are represented.

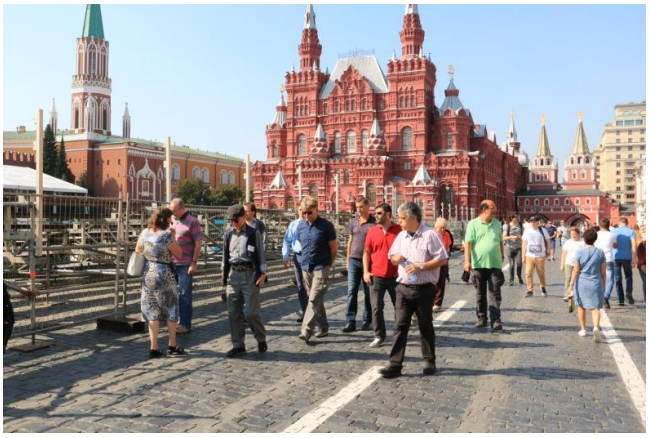

Figure 7: On the Red Square.

The Workshop Dinner was held in the restaurant "Taras Bulba" placed on the street Piatnitskaya in the old part of Moscow in downtown (Fig.8).

Figure 8: Workshop Dinner: Restaurant "Taras Bulba"

After the Workshop Dinner, the participants admired the view of evening Moscow from a viewing platform on the Vorob'ev Hills near the Moscow State University (Fig. 9).

The business meeting of ISC was held on 06.09.2018. The planned rotation of ISC member was realized and Prof M. Nagatsu was replaced by Prof. H. Toyoda as a representative of Japan. Taking into account the important contribution of Prof. M. Nagatsu in the success of the Workshop, he was elected the Honorary Member of ISC. Prof. E. Benova was elected the Chairman of the ISC for the period 2019-2021 and the Chairman of the next Workshop (MD-11). MD-11 will be held in Bulgaria in 2021 (Fig.10).

Figure 9: View of stadium "Luzhniki" from the viewing platform.

Figure 10: Elected Chairman of ISC Prof. Eugenia Benova

Further information:

http://www.fpl.gpi.ru/md-10

About the author

Yuri A. Lebedev was born in USSR. His education includes engineer in electronics (1968) and physicist (1974). He obtained his PhD degree in 1977 and degree of Doctor of Sciences in plasma physics in 1993. He has over 45 years of research experience in low temperature plasma, electric gas discharges, microwave plasma, plasma chemistry, plasma diagnostics and modeling. He is a member of editorial boards of several journals and published over 350 papers, editor and co-author of 9 books. He is a member and one of the founders of the International Scientific Committee on Microwave Discharges: Fundamentals and Applications (Chairman 1997-2000, 2003-2006, 2009-2012, 2015-2018), Deputy Chairman of the Scientific Council of the Russian Academy of Sciences on Physics of Low Temperature Plasma, Member of the Executive Boards of the United Physical Society of the Russian Federation and of the Moscow Physical Society, the Chairman/Member of Advisory and Program Committees of various conferences and schools on Low temperature Plasma Physics and Plasma Chemistry. His affiliation since 1971 is the Topchiev Institute of Petrochemical Synthesis of the Russian Academy of Sciences, Moscow, Russia. Since 1996 he is a head of the Laboratory of Plasma Chemistry and Physical Chemistry of Pulse Processes.

Highlights of the JEMEA2018 Symposium in Japan

Naoki Shinohara [1, 2]

[1]President of JEMEA (Japan Society of Electromagnetic Wave Energy Applications)
[2]Research Institute for Sustainable Humanosphere, Kyoto University
Gokasho, Uji, Kyoto, 6110011, Japan
Contact Email: shino@rish.kyoto-u.ac.jp

JEMEA, Japan Society of Electromagnetic Wave Energy Applications, is a Japanese scientific society which promotes science and technology of electromagnetic wave energy applications. The aim was to disseminate the advances in basic and applied electromagnetic energy, and to spread a science culture to contribute to the development of industry and the improvement of life. JEMEA was established based on the Institute of Electromagnetic Wave Application, Japan (IEAJ) and Microwave Technology Forum on August 31, 2006. JEMEA was certified NPO (Registered Non-Profit Organization) by the Tokyo Metropolitan Government on May 23, 2007, and registered as NPO on June 1, 2007.

Every year JEMEA organizes a symposium and several workshops on electromagnetic wave energy applications. Some working groups, for e.g. computer simulation of the electromagnetic waves, safety issues, education, standardization, etc. are also set up within JEMEA.

On November 15th – 16th, the 12th JEMEA symposium was held in Kitakyushu international conference hall in Japan. The general chair of the JEMEA symposium was Prof. Shokichi Ouchi of Kyushu Inst. of Tech. The total number of accepted papers was 87 (58 orals in two parallel sessions, 25 posters, 2 keynote speeches from oversea, and 2 speeches as award ceremony). There were excellent and interesting presentations which resulted in fruitful discussions (Fig. 1 and 2). Keynote speakers were Prof. Gregory B. Dudley of West Virginia University, US, whose paper title was “Selective microwave heating of organic reaction mixtures”, and Prof. Cristina Leonelli of University of Modena and Reggio Emilia, Italy, whose paper title was “An overview of AMPERE activities and members research in Europe” (Fig. 3). Apart from the keynote talks, all other papers were presented in Japanese.

Figure 1: Conference Room

Figure 2: Poster Session

In every symposium, JEMEA's review committee chooses JEMEA best paper award from the orals presentations and the JEMEA best poster award. In 2018, we chose the following award winners:

JEMEA Best paper award:

Highest award

- "Microwave Heating of Metal Nanoparticles supported on Metal Oxides" by T. Ano, Tokyo Inst. of Tech., et al.

Award of excellence

- "Preparation and Particle Size Control of Rh Nanoparticles via Microwave-assisted Alcohol Reduction" by Y. Nishida, Oita Univ., et al.

JEMEA Best poster award:

- "Electronic component mounting on low heat resistance substrate by using magnetic field heating of microwaves" by T. Nakamura, The National Institute of Advanced Industrial Science and Technology (AIST)
- "Degradation of methyl orange by Au/TiO2 photocatalytic nanoparticles prepared using microwave heating" by Y. Arimura, Kindai Univ., et al.
- "Pressurized microwave degradation of waste bathtub resin and recycling" by T. Hatanaka, Sojo Univ., et al.

JEMEA is supported by a number of companies which promote the use of electromagnetic wave applications. In the JEMEA symposium, 14 companies exhibited their products (Fig.4). They introduced their products in a special oral session dedicated to industry. The companies exhibiting were:

- Astech Corp.
- Amil Co., Ltd.
- Anton Paar Japan K.K.
- Anritsu Meter Co., Ltd.
- M3 Laboratory Co., Ltd.
- Orient Microwave. Corp.
- KESCO (Keisoku Engineering System Co., Ltd.
- Shikoku Instrumentation Co., Ltd.
- Tokyo Rikakikai Co., Ltd.
- Fuji Electronic Industrial Co., Ltd.
- Milestone General K.K.
- Micro Denshi Co., Ltd.
- Mitsubishi Electric Corporation
- Chengdu Wattsine Electronic Technology (China)

Figure 3: Prof. Leonelli as Keynote Speaker

Figure 4: Exhibition Hall with 14 Companies

The total number of attendees was 169 (72 from universities, 84 from industry, and 13 from government departments). 96 participants are JEMEA members, 13 participants were technical co-sponsorship members from industry, while 8 foreign attendees did represent 6 different countries.

Additionally, there were 2 events in series to promote the electromagnetic wave energy applications in the JEMEA symposium. One was a Short Course on Nov. 14th at the same conference hall, whose title was “What we should understand for safe use of microwave energy”. To ensure that research and technical development by using electromagnetic wave energy continues well into the future, it's a well -known fact that paying full attention to safety measures is very important. Of

course, we can make some prediction of what is needed and the required experimentation, since we have our own accumulated experience. We can also use void simulation techniques to avoid costly mistakes. But without knowing, we may encounter unpredictable dangers or accidents. This short course aimed for solutions on most troubling aspects about electromagnetic wave energy application technology from the standpoint of Heinrich's law, known as "Hiyari-hatto" (unreported occurrences in English).

For the short course, we invited 3 speakers who are the experts in safety of electromagnetic waves, electromagnetic wave energy applications, and regulations related to microwave heating. In addition to 3 invited speakers, we have chosen 6 speakers from the public. It is not uncommon for people who are in charge of research or development with electromagnetic wave energy to experience errors, failures or accidents. JEMEA welcomed open-application speakers who showed their experiences within 15 min. We chose various afflictions (e.g. university, company, laboratory) and organized a "Hiyari-hatto" session.

The number of participants in the short course was 64 (43 JEMEA members, 21 non-JEMEA members which includes 4 technical co-sponsorship members. The audience enjoyed talks and a demonstration of a microwave oven.

The other series event on Nov. 17th was a public program offered to the public about the use of electromagnetic wave energy. This was an open program for everyone. Speakers were mainly from JEMEA. 5 JEMEA members introduced latest information about microwave energy. Additionally, we invited Dr. Shoko Murakami, the famous expert in microwave cooking. She gave a demonstration of her original cooking. 53 citizens attended and enjoyed this program.

The total number of attendees of all three events was 287. The 12th JEMEA symposium and related events were successful finished. The 13th JEMEA Symposium (Sympo2019) will be held from Oct. 30th - Nov.1st, 2019 at AIST Tsukuba, Ibaraki Prefecture, Japan. Dr. Hiroki Shimizu is the general Chair of Sympo2019 and will announce details in early February, 2019. We welcome your attendance to JEMEA symposium 2019.

Naoki Shinohara received the B.E. degree in electronic engineering, the M.E. and Ph.D (Eng.) degrees in electrical engineering from Kyoto University, Japan, in 1991, 1993 and 1996, respectively. He was a research associate in the Radio Atmospheric Science Center, Kyoto University from 1996. He was a Research Associate of the Radio Science Center for Space and Atmosphere, Kyoto University by joining the Radio Atmospheric Science Center from 2000, and there he was an Associate Professor since 2001. He was an associate professor in Research Institute for Sustainable Humanosphere, Kyoto University by joining the Radio Science Center for Space and Atmosphere since 2004. From 2010, he has been a Professor in Research Institute for Sustainable Humanosphere, Kyoto University. He has been engaged in research on Solar Power Station/Satellite and Microwave Power Transmission system. He is IEEE MTT-S Technical Committee 26 (Wireless Power Transfer and Conversion) vice chair, IEEE MTT-S Kansai Chapter TPC member, IEEE Wireless Power Transfer Conference advisory committee member, international journal of Wireless Power Transfer (Cambridge Press) executive editor, Radio Science for URSI Japanese committee member, technical committee on IEICE Wireless Power Transfer, communications society chair, Wireless Power Transfer Consortium for Practical Applications (WiPoT) chair, and Wireless Power Management Consortium (WPMc) chair

Ricky's Afterthought:

Silicon Gunn Effect

A.C. (Ricky) Metaxas
Life Fellow St John's College Cambridge UK
Email: acm33@cam.ac.uk

As it is well known, gallium arsenide (GaAs) is at the heart of the Gunn Effect which is used for the generation of microwaves. It was discovered by J.B.Gunn in 1962 at IBM in the USA. Put simply, as the voltage in a Gunn diode increases the current increases but at a certain point the mobility of the electrons starts decreasing producing a negative resistance and it is this inherent property which enables oscillators to be produced at high frequencies. Fig.1 shows a typical I-V characteristic depicting such an effect.

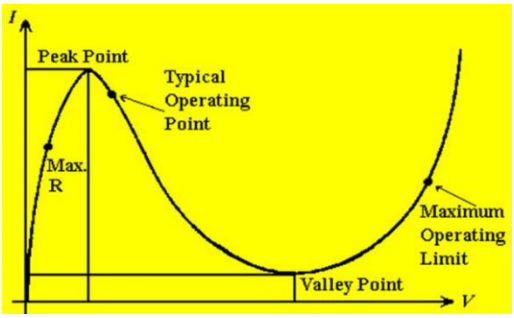

Fig.1: Gun effect showing a typical operating point

Gunn Diodes consist only of n-type semiconductors unlike other diodes that have both n and p-types. It is termed a diode because it has two terminals. They do not conduct current only in one direction and do not rectify alternating currents hence it is best to refer to these as Transfer Electron Devices. Apart from GaAs other materials are used such as Indium Phosphide, InP. It is necessary to use n-type material because the Transferred Electron effect is only applicable to electrons and not to holes found in a p-type material.

The principle behind its operation lies behind the discovery by British physicists Brian Ridley, Tom Watkins and Cyril Hilsum, known as the Ridley-Watkins-Hilsum theory, that some semiconductors could exhibit negative resistance thus opening the possibility of the generation of microwaves.

GaAs Gunn diodes are used in radio links, speed radar traps, automatic door openers, antilock brakes and airborne collision avoidance radar systems.

But GaAs, as a material, is expensive so a collaborative research project from the Physics Dept at Chalmers, Sweden, Dept of Electrical Engineering and Computing Science at Texas A&M University, Kingsville, USA, Dept of Electrical and Computing Engineering, University of Waterloo at Ontario, Canada and the Dept of Electrical Engineering University of Washington, at Seattle, USA, considered whether cheaper materials may exhibit a Gunn-type Effect. Indeed the researchers using Density Functional Theory, Semi-Empirical 10 Orbital (sp3d5s*) Tight Binding and Ensemble Monte Carlo computer models, established that tiny ***silicon nanowires*** with diameters of 3.1nm and when an electric field of 5 kV/cm is applied, a Gunn-type Effect is produced when stretched presenting the possibility that microwaves can be generated with a material which is abundant and far cheaper that GaAs. However, it is noted that about 100000 bundled together would be needed to produce a product as large as a human hair! Although that is a no mean feat, nanofabrication techniques are available which bundle together bulk silicon into nanowires and therefore are capable of producing a Gunn Effect. The researchers believe that the stretching mechanism could act as a switch to turn the Effect on and off, and possibly vary the frequency, which would render this device suitable for a host of new applications.

For further reading

For more detailed information regarding this research visit the following link:
https://www.nature.com/articles/s41598-018-24387-y

AMPERE Medal 2019

Recipients of the MEDAL so far ware Mr Bernard Krieger, USA, (2015) and Professor Yoshio Nikawa, Japan (2017).

Applications are now open for nominating a person to be awarded the 2019 AMPERE MEDAL at our next conference in Valencia in September 2019. Nominees do not have to be members of AMPERE. The Honorary President is excluded from being nominated.

A guideline regarding the stature of person eligible for the AMPERE MEDAL is as follows:

"The AMPERE MEDAL is an award for outstanding contributions in the field of Industrial Microwave or RF Heating, first instigated at the 2015 AMPERE conference in Kraków. It is the highest honour that our organisation can bestow and goes to an individual who has gravitas and has worked tirelessly promoting the use of RF/microwave energy in academe, industry or related areas. It is not intended for a young researcher who is in the process of establishing a good reputation in the fields stated above.

The MC decided on the following timetable:

- Each AMPERE member, should they wish, is asked to nominate ONE person and together with the his/her email address to e-mail it to amperemedal@ampereeurope.org by 30 March 2019.
- Nominees are sent a form to complete and sent to amperemedal@ampereeurope.org by 1st May 2019.
- President and Honorary President e-mail members of the MC by 15 May 2019 the names of the nominees and attach their completed forms.
- Each MC member chooses ONE nominee and sends this name to both President and Honorary President by 15 June 2019.
- President and Honorary President receive the votes from MC and declare the winner. MC is informed of the result.
- Winner receives the inscribed MEDAL at the Gala dinner in September 2019.

Of all the nominees considered, only those that have registered and are present at the Gala dinner in Valencia will be eligible to receive this award.

AC Metaxas
January 2019

Upcoming Events

The 17th International Conference on Microwave and High Frequency Heating: AMPERE 2019 is the largest event in Europe dedicated to scientific and industrial applications of microwave and radiofrequency power systems. The conference presents the status and trends in the multidisciplinary fields of microwave and radiofrequency heating, dielectric properties, material processing, high power systems and technologies.
The AMPERE conference is a unique opportunity for the presentation and discussion of the most recent advances in the microwave technology and its applications. The conference provides many opportunities to researchers and engineers from academia and industry to exchange innovative ideas, networking, discuss collaborations and to meet with international experts in a wide variety of specialties of microwave and high frequency technologies at both scientific and industrial scale.
Deadline for submission of abstracts is 10 March 2019
Website: http://ampere2019.com/

Conference Venue
The conference will be held in the The Polytechnic City of Innovation (CPI). The CPI is the Science Park of the Universitat Politècnica de València (UPV). The Science Park is conceived as a space, not only in physical terms, to connect university, business and society in order to streamline the generation of knowledge-intensive activities.

Scope and Topics
A broad range of microwave and radio frequency related topics, from materials and technologies to high power systems and applications will be addressed in all their aspects: theory, simulation, design, measurement and applications. Topics include, but are not limited to:

- Energy Production by Microwaves (including renewable energy and chemicals)
- Plasma processing induced by microwaves (CVD, cleaning, nanoparticles...)
- Microwave and High Frequency Material interaction
- Dielectric and Magnetic Material Properties and Measurements
- EM Modelling and Numerical Techniques
- Design of Microwave Applicators and Components
- Solid State Microwave Technology
- Microwave and High Frequency Sources and Power Supply
- Microwave Industrial Equipment and Scale-up
- Microwave Chemistry
- Food Processing
- Microwave Packaging
- Medical and Biological Applications
- Radiation Safety and Standards
- Trends in Microwave Processing

EuMCE 2019, 1st European Microwave Conference in Central Europe
13th - 15th May 2019 Prague, Czech Republic
The European Microwave Association (EuMA) is launching the European Microwave Conference in Central Europe, with associated Workshops and an Exhibition. EuMCE is a new series of events, modelled on European Microwave Week that is to complement the existing conferences in the region. It will be held every two years, alternating with MIKON and visiting the major cities of Central Europe.
Website: https://www.eumce.com/

HES 19 – International Symposium on Heating by Electromagnetic Sources
22nd - 24th May, 2019, Padova, Italy
The latest results of research and industrial development activities in the field of: Induction, Conduction, Dielectric, Microwaves Heating and EPM (Electromagnetic Processing) will be presented and discussed by researchers, international experts and engineers from industry**.**
Website: http://hes19.dii.unipd.it/

IMS2019, International Microwave Symposium
2nd -7th June, 2019, Boston, USA
The IEEE Microwave Theory and Techniques Society's 2019 IMS Microwave Week will be held 2-7 June 2019 in Boston, Massachusetts. IMS Microwave Week consists of three related conferences offering technical sessions, interactive forums, plenary and panel sessions, workshops, short courses, industrial exhibits, application seminars, historical exhibits, and a wide variety of other technical and social activities including a guest program. The International Microwave Symposium (IMS) is the centerpiece of the Microwave Week technical program, which includes the Radio Frequency Integrated Circuits Symposium (RFIC) and the Automatic Radio-Frequency Techniques Group Conference (ARFTG). With over 10,000 participants and 1000 industrial exhibits of state-of-the-art microwave products, IMS Microwave Week is the world's largest gathering of Radio Frequency (RF) and microwave professionals and the most important forum for the latest research advances and practices in the field.
Website: https://ims-ieee.org/

IMPI's 53rd Annual Microwave Power Symposium
18th – 20th June8-20, 2019 Las Vegas, Nevada, USA
The International Microwave Power Institute invites scientists, engineers, industry professionals and users to submit papers in all areas of research, development, manufacture, engineering, specification and use of microwave and radio frequency energy systems for non- communication applications, including industrial microwave and RF, solid state, food technology, plasma, chemical, material processing, and new emerging technologies.
Website: http://impi.org/symposium-short-courses/

European Microwave Conference 2019
1st – 3rd October 2019, Paris France
The 49th European Microwave Conference (EuMC) represents the main event in the European Microwave Week 2019, the largest event in Europe dedicated to microwave components, systems and technology.
The EuMC is a premier event to present the status and trends in the fields of microwave, millimetre-wave and terahertz systems and technologies.
Website: https://www.eumweek.com/conferences/eumc.html

Public Funded Projects within the AMPERE Community

TOMOCON

Smart Tomographic Sensors for Advanced Industrial Process Control

Project type:
H2020-MSCA-ITN-2017
Marie Skłodowska-Curie Action
Innovative Training Networks

Grant agreement ID: 764902

Start date: September 2017
End date: August 2021

A decisive gap in the process industry is the lack of qualified distributed process parameter measurements for optimal control. Process tomography is a ground-breaking technology to bridge this gap. Just with the recent development in high power massive parallel computing this technology has gained the required real-time capability. TOMOCON as a European network of leading academic and industrial partners from different sectors dedicates its efforts in research and training towards development of tomography-based industrial process control. With that it shall generate new scientific and technical knowledge in this emerging field; develop and demonstrate new technological solutions of advanced industrial control by tomographic sensors; align tomography-based process control with concepts of knowledge-based control, big data analysis and advanced human-machine interfaces; and enhance the scientific and transferable skills of early stage researchers to meet future needs of the industry. Together with world-leading industrial sensor and control solution providers, process engineering and production companies TOMOCON shall demonstrate the functionality of tomography-assisted process control in four industry-relevant demonstration cases, which serve as benchmarks to demonstrate improvements in energy and resource efficiency as well as product quality. That is control of inline fluid separation, control of microwave drying processes, control of continuous metal casting, and control of batch crystallization processes. The microwave group at KIT is the demonstration leader for a microwave tomographic sensor and use thereof for control of a microwave assisted and continuous drying process of porous materials.

For further information:

www.tomocon.eu

https://cordis.europa.eu/project/rcn/211526/factsheet/en

SIMPLIFY

SONICATION & MICROWAVE PROCESSING OF MATERIAL FEEDSTOCK

Sonication and Microwave Processing of Material Feedstock (SIMPLIFY) responds to the EU Horizon 2020 call SPIRE-02-2018 and is a 48-month innovation action in which leading European industries and university groups in process intensification, ultrasound, microwave, multiphase processes, polymerization and crystallization team up to address the domain of electrification of chemical industry. In four years (starting date: November 1, 2018), a consortium of 11 European organizations, led by KU Leuven, will focus on intensified processes, where alternative energy sources enable flexible continuous technologies to achieve localized ultrasound and microwave actuation of multiphase, flow reactors powered by electricity from renewable sources for the purpose of high-value product synthesis.

At the core of the SIMPLIFY project are the three case-studies, serving as representatives for process classes of high importance in the chemical industry: one in the domain of reactive extrusion (class of processes involving viscous streams), the other two in the domain of reactive crystallization (class of processes involving suspensions). Each of these case-studies is of interest to one industrial end-user in the project. These end-users are in charge of the industrial validation and demonstration on-site. The three case-studies are supported by both generic and applied research on the enabling technologies: US, MW and process control. In addition to the process technology-oriented activities, the sustainability and techno-economic improvement are investigated that can be reached by transitioning from a batch process to an US/MW-assisted continuous process. This activity supports in making technical decisions of where the processes can benefit most from US and MW activation.

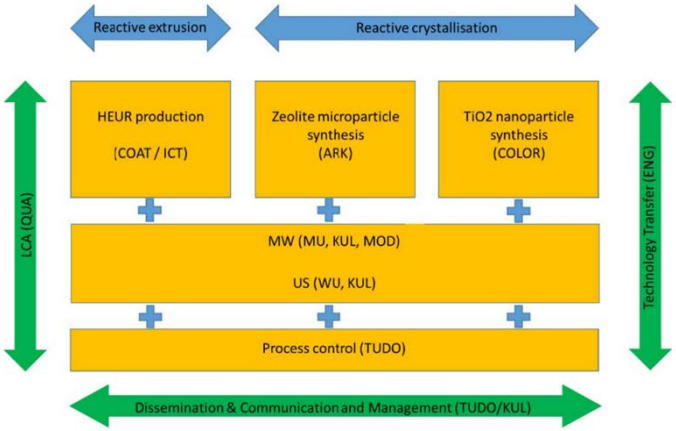

For further information:

https://www.spire2030.eu/simplify

Call for Papers:

Special Issue on Localized Microwave-Heating (LMH)

The open-access Journal ***materials*** published by MDPI (https://www.mdpi.com/journal/materials) has launched a new Special Issue (SI), titled:

"Localized Microwave-Heating (LMH): Materials, Phenomena, and Applications"

This SI is dedicated to LMH and its various aspects, in a unified paradigmatic approach (see Pages 1-8 here), including fundamental mechanisms and enabling material properties, LMH phenomena in various fields, and potential applications.

The topics of interest include:

- Temperature-dependent material properties
- Localized microwave-heating effects and hotspot formation
- Thermal-runaway instabilities
- Melting, cracking and drilling
- Powder heating and sintering
- Microwave chemistry
- Plasma ignition and localization effects
- Combustion
- Biological effects, microwave hazards
- Medical treatments, tissue ablation
- Microwave engineering, solid-state generators
- Any other aspect of LMH

Manuscripts can be submitted until the deadline (Feb. 29, 2020). All papers will be peer-reviewed. Accepted papers will be published continuously in the journal (as soon as accepted) and will be listed together on the special issue website.

For further information

This SI is now open for submission online at:
https://www.mdpi.com/journal/materials/special_issues/Localized_Microwave_Heating

or directly call the Guest Editor, Prof. Eli Jerby, at jerby@eng.tau.ac.il

About AMPERE Newsletter

AMPERE Newsletter is published by AMPERE, a European non-profit association devoted to the promotion of microwave and RF heating techniques for research and industrial applications (http://www.AmpereEurope.org).

Call for Papers

AMPERE Newsletter welcomes submissions of articles, briefs and news on topics of interest for the RF-and-microwave heating community worldwide, including:

- Research briefs and discovery reports.
- Review articles on R&D trends and thematic issues.
- Technology-transfer and commercialization.
- Safety, RFI, and regulatory aspects.
- Technological and market forecasts.
- Comments, views, and visions.
- Interviews with leading innovators and experts.
- New projects, openings and hiring opportunities.
- Tutorials and technical notes.
- Social, cultural and historical aspects.
- Economical and practical considerations.
- Upcoming events, new books and papers.

AMPERE Newsletter is an ISSN registered periodical publication hence its articles are citable as references. However, the Newsletter's publication criteria may differ from that of common scientific Journals by its acceptance (and even encouragement) of news in more premature stages of on-going efforts.

We believe that this seemingly less-rigorous editorial approach is essential in order to accelerate the circulation of ideas, discoveries, and contemporary studies among the AMPERE community worldwide. It may hopefully enrich our common knowledge and hence exciting new ideas, findings and developments.

Please send your submission (or any question, comment or suggestion in this regard) to the Editor in the e-mail address below.

AMPERE-Newsletter Editor

Guido Link, Karlsruhe Institute of Technology, Karlsruhe, Germany, E-mail: guido.link@kit.edu

Editorial Advisory Board

AMPERE Disclaimer

AMPERE Newsletter

ISSN 1361-8598

https://www.ampereeurope.org/newsletter/